Improved therapeutic efficacy of decorin expressing oncolytic adenovirus driven by cancer- and tumor microenvironment-specific promoter in pancreatic cancer

Yan Li

The Graduate School

Yonsei University

Graduate Program for Nanomedical Science

Improved therapeutic efficacy of decorin expressing oncolytic adenovirus driven by cancer- and tumor microenvironment-specific promoter in pancreatic cancer

Directed by Professor In-Hong Choi

The Doctoral Dissertation
Submitted to the Graduate Program for Nanomedical
Science and the Graduate School of
Yonsei University in partial fulfillment of the
Requirements for the degree of
Doctor of Philosophy

Yan Li

February 2017

연세대학교
YONSEI UNIVERSITY

This certifies that the doctoral dissertation of Yan Li is approved.

Thesis Supervisor: In-Hong Choi

Thesis Committee Member#1: Jeon-Soo Shin

Thesis Committee Member#2: Seung Woo Park

Thesis Committee Member#3: Mijin Yun

Thesis Committee Member#4: Chae-Ok Yun

The Graduate School

Yonsei University

February 2017

ACKNOWLEDGEMENTS

설렘과 두려움을 안고 시작했던 학위과정, 이제 비로소 모든 과정을 마치며 지난 시간을 되돌아봅니다. 처음 박사과정에 발을 디딘 날로부터 지금 이 순간까지의 시간은 저에게는 학문의 길 뿐 아니라 생장의 시간이었고 감사한 삶이었습니다. 그 시간 동안 옆에서 도와주신 많은 분들이 아니었다면 어떻게 지금 이 순간이 있었을지 상상이 가지 않습니다. 이렇게 결실을 맺기까지 부족한 저를 지도해주신 윤채옥 교수님, 교수님을 향한 감사의 마음을 어떻게 글로 다 표현할 수 있을까요. 교수님은 제 안의 작은 것을 알아봐 주셨고, 한 의사로서의 소양 뿐 아니라 삶의 자세에 대한 가르침을 주셨습니다. 교수님의 열정과 지도 덕분에 학위과정을 끝까지 마칠 수 있었습니다. 박사과정 동안 교수님의 가르침을 통해 유전자치료란 학문에 매력을 느낄 수 있었고, 학문에 대한 끝없는 갈증과 연구에 매진하시는 모습을 통해 많은 깨달음을 얻었습니다. 진심으로 감사 드립니다. 그 동안 주신 가르침 잊지 않고 살아가겠습니다. 그리고 흔쾌히 지도교수를 허락해주신 최인홍 교수님, 논문 심사를 맡아주시고, 소중한 충고와 조언을 아끼지 않으신 신전수 교수님, 박승우 교수님, 그리고 윤미진 교수님께 깊은 감사를 드립니다. 학문을 사랑하는 학자로서의 모습을 통해 항상 귀감이 되어주시는 생명공학과 교수님들께도

감사를 드립니다.

유전자치료 연구실에 입학한 이후로 함께하며 도움을 주셨던 선배님들과 후배님들께 역시 깊은 감사를 드립니다. 존경스러운 민정 언니, 힘이 되어준 지훈 오빠, 안식처가 되어준 아름 언니, 능력 있는 정우 오빠, 배울점이 정말 많은 정선 언니, 항상 진심으로 다가와준 일규 오빠, 많은 가르침을 주신 송남 오빠, 의지가 된 태진 오빠, 유능한 오준이, 감성적인 지성이, 똑부러진 혜원이, 해피바이러스 성경이, 듬직한 언주, 선배 같은 후배 핑크빛 유진이, 부지런한 초희, 엉뚱한 효민이, 능력자 kasala 박사님, 분위기 메이커 수정이, 보고싶은 후배 종현이, 나노팀 선장 수환이, 아픈 손가락 정은이, 살림꾼 보경이, 남자다운 원식이, 섬세한 득영이, 도움을 많이 준 진우, 타국에서 고생하는 춘영이, 일 잘하는 태극이, 책임감 있는 하늘이, 기대주 용현이와 혜령이 모두 진심으로 감사드립니다.

무엇보다도 저에 대한 걱정으로 하루하루를 살아가시고 계신 사랑하는 부모님께 감사드립니다.

이 외에 제가 미처 언급하지 못한 고마운 분들이 너무나 많습니다. 그 분들의 이름을 모두 새기지 못함을 죄송하게 생각하며, 대신 제 깊은 감사의 말로 이 글을 마칩니다. “진심으로 감사드립니다”

저자 씀

TABLE OF CONTENTS

LIST OF FIGURES

ABSTRACT

Improved therapeutic efficacy of decorin expressing oncolytic adenovirus driven by cancer- and tumor microenvironment-specific promoter in pancreatic cancer

Yan Li

Graduate Program for Nanomedical Science
The Graduate School
Yonsei University

(Directed by Professor In-Hong Choi)

Pancreatic cancer is a leading cause of cancer-related death. Desmoplastic pancreatic tumors exhibit excessive extracellular matrix (ECM) and are thus highly resistant to anticancer therapeutics, since the ECM restricts drug penetration and dispersion. Here, we designed and generated two hypoxia-responsive and cancer-specific hybrid promoters, HmTE and HEmT. Transgene expression driven by each hybrid promoter was markedly higher under hypoxic conditions than normoxic conditions. Moreover, HEmT-driven transgene expression was highly cancer-specific and was superior to that of HmTE-driven expression. A decorin-expressing oncolytic adenovirus (Ad; oHEmT-DCN)

replicating under the control of the HEmT promoter induced more potent and highly cancer-specific cell death compared with its cognate control oncolytic Ad, which harbored the endogenous Ad E1A promoter. Moreover, oHEmT-DCN exhibited enhanced antitumor efficacy compared with both the clinically approved oncolytic Ad ONYX-015 and its cognate control oncolytic Ad lacking DCN. oHEmT-DCN treatment also attenuated the expression of major ECM components, such as collagen I/III, elastin, and fibronectin, and induced tumor cell apoptosis, leading to extensive viral dispersion within orthotopic pancreatic tumors and pancreatic cancer patient-derived tumor spheroids. Collectively, these findings demonstrate that oHEmT-DCN exhibits potent antitumor efficacy by degrading the ECM and inducing apoptosis in a multifunctional process. This process facilitates the dispersion and replication of oncolytic Ad, making it an attractive candidate for the treatment of aggressive and desmoplastic pancreatic cancer.

Key word: Oncolytic adenovirus; Pancreatic cancer; Decorin; Hypoxia; Desmoplasia; Cancer-specific promoter; Extracellular matrix

Improved therapeutic efficacy of decorin expressing oncolytic adenovirus driven by cancer- and tumor microenvironment-specific promoter in pancreatic cancer

Yan Li

Graduate Program for Nanomedical Science
The Graduate School
Yonsei University

(Directed by Professor In-Hong Choi)

I. INTRODUCTION

Pancreatic cancer is the fourth leading cause of cancer-related death in Europe and the United States [1]. Only 10-20% of all patients with pancreatic cancer are resectable at presentation. The US National Cancer Institute recently reported that the overall 5-year relative survival rate for 2002-2008 was 5.8%, and nearly 90% of all patients were dead 1 year after diagnosis, with a median survival of less than 6 months [2, 3]. One experimental treatment option of particular interest for pancreatic cancer is oncolytic virotherapy, which utilizes viral vectors to preferentially replicate in tumor cells and induce cancer cell death. Among the various viral vectors that have been tested, adenovirus (Ad) has been most extensively utilized in gene therapy applications, and sufficient

data from randomized clinical trials support its safety in patients [4-6]. Although oncolytic Ad-mediated cancer gene therapy is highly promising, significant therapeutic efficacy of oncolytic Ad for the treatment of localized tumors has not yet been achieved in clinical trials; thus, further improvements are needed [7, 8].

Hypoperfusion and desmoplasia are two prominent features of pancreatic cancer that attenuate the therapeutic efficacy of cancer therapeutics [9]. Aberrant extracellular matrix (ECM) functions as a protective layer that prevents drug penetration and diffusion into the pancreatic tumors, contributing to poor disease management by conventional treatment modalities. Furthermore, hypoxia, a condition characterized by oxygen deprivation caused by abnormal microcirculation and vascularization in the tumor microenvironment, promotes cancer progression and attenuates the therapeutic efficacy of oncolytic Ad by suppressing viral replication through downregulation of Ad E1A protein expression [10-12].

Decorin (DCN), a ubiquitous component of the ECM, is preferentially found in association with collagen fibrils. Furthermore, DCN regulates the production of other ECM components by blocking the activity of transforming growth factor-β (TGF-β), which is a major inducer of desmoplasia in pancreatic tumors [13]. We previously demonstrated that oncolytic Ad-mediated

intratumoral expression of DCN can drive degradation of the ECM and inhibit ECM production, thereby enhancing viral penetration and dispersion within solid tumors and making DCN a promising therapeutic gene for the treatment of desmoplastic tumors [14].

A successful oncolytic Ad-mediated cancer gene therapy requires good cancer-specificity, since ectopic replication of Ad at nontarget tissues will result in cytotoxicity. In this regard, numerous studies have been conducted with the aim of achieving selective replication of Ad in a cancer cell-specific manner. A particularly promising approach for endowing cancer-specificity to replication-competent Ad is to restrict viral replication to cancer cells by replacing the endogenous Ad promoter with a cancer cell-specific promoter. Among the cancer-specific promoters, both the E2F and human telomerase reverse transcriptase (hTERT) promoters have demonstrated good cancer specificity [15, 16]. We previously showed that oncolytic Ad replicating under the control of a modified hTERT (mTERT) promoter containing additional c-Myc and Sp1 binding sites replicates more efficiently and preferentially in tumor cells than its cognate control Ad replicating under the wild-type hTERT promoter, resulting in more potent Ad E1A-mediated apoptosis and viral cytolysis in a cancer-restricted manner [17]. However, the therapeutic effect of oncolytic Ad in the hypoxic region of the tumor nest was still insufficient, since

hypoxia directly impacts the therapeutic efficacy of oncolytic Ad by suppressing viral replication through attenuation of Ad E1A protein expression [10-12].

To overcome this hypoxia-induced downregulation of Ad E1A expression in solid tumors and to enhance their cancer-selective promoter activity, we designed and generated two different enhancer/promoter hybrids that incorporate 6 copies of the hypoxia response element (HRE) upstream of either the E2F or modified human telomerase reverse transcription (mTERT) promoter. This strategy generated an HRE-mTERT-E2F hybrid promoter (HmTE) and an HRE-E2F-mTERT hybrid promoter (HEmT). In this study, we demonstrate that DCN-expressing oncolytic Ad replicating under the control of the HEmT hybrid promoter (oHEmT-DCN) exerts potent tumoricidal effects by efficaciously and preferentially replicating in both hypoxic and normoxic regions of highly desmoplastic pancreatic tumors.

II. MATERIALS AND METHODS

Cell lines and cell culture

All cell lines with the exception of normal pancreatic cells (NPC), which was maintained in prigrow I medium, were cultured in Dulbecco's modified Eagle's medium (DMEM; GIBCO BRL, Grand Island, NY) supplemented with 10% fetal bovine serum (GIBCO BRL) and penicillin-streptomycin (100 IU/mL, GIBCO BRL). The HEK293 (human embryonic kidney cell line expressing the Ad E1 region), A549 (human lung cancer cell line), MIA PaCa-2 and PANC-1 (pancreatic cancer cell lines), and human dermal fibroblast (HDF; normal fibroblast cell line) cell lines were purchased from the American Type Culture Collection (ATCC, Manassas, VA). The NPC cell line was purchased from Applied Biological Materials (ABM, Richmond, Canada). All cell lines were maintained at 37°C in a humidified atmosphere at 5% CO_2.

Animal studies

Six to eight-week-old male athymic nude mice were purchased from Charles River Korea (Sungnam, Korea) and maintained in a laminar air flow cabinet under specific pathogen-free environment. All facilities were approved

by AAALAC (Association for Assessment and Accreditation of Laboratory Animal Care). All of the animal experiments were conducted according to the institutional guidelines established for the Hanyang University Institutional Animal Care and Use Committee.

Construction of the Ad vectors

To generate the two different cancer-specific hybrid promoters, HRE/mTERT/E2F (HmTE) and HRE/E2F/mTERT (HEmT), the HRE enhancer, E2F, and the mTERT promoter were inserted into pDE1sp1B, thereby generating pDE1sp1B-HmTE and pDE1sp1B-HEmT [10, 17, 18]. To construct E1 shuttle vectors expressing green fluorescent protein (GFP) under the control of the modified cancer-specific promoters (HmTE and HEmT), the sequence encoding GFP was subcloned from pEGFP-N1 using *Xho* I/*Afl* II. This GFP gene was then ligated into pDE1sp1B/HmTE and pDE1sp1B/HEmT cut with the same restriction enzymes, thereby generating the pDE1sp1B/HmTE-GFP and pDE1sp1B/HEmT-GFP Ad E1 shuttle vectors. The Ad E1 shuttle vectors were linearized by *Xmn* I digestion, whereas the Ad vector dE1-k35 was linearized with *Bst*B I digestion. The linearized Ad shuttle vectors were cotransformed into *Escherichia coli* BJ5183 cells with *Bst*B I-digested dE1-k35 to allow for homologous recombination. The resultant homologously

recombined Ad plasmid was digested with *Pac* I and transfected into HEK293 cells to generate the replication-incompetent Ads, dHmTE-GFP and dHEmT-GFP. GFP-expressing Ad under the control of the cytomegalovirus (CMV) promoter (dCMV-GFP) was used as a control [19, 20].

To create an oncolytic Ad replicating under the control of the HEmT promoter, a template Ad plasmid consisting of the E1B 19kDa region-deleted E1 shuttle vector (pDE1sp1B/Rd19) harboring the retinoblastoma binding sites of mutant E1A was used [21, 22]. Initially, the HEmT promoter was inserted into pDE1sp1B/Rd19, thereby generating the pDE1sp1B/HEmT-Rd19 Ad E1 shuttle vector. To create a DCN-expressing replicating Ad vector, the sequence encoding DCN was subcloned from pCA14/DCN using *Bgl* II into pDE1sp1B/HEmT-Rd19, thereby generating the pDE1sp1B/HEmT-Rd19/DCN Ad E1 shuttle vector. These Ad E1 shuttle vectors (pDE1sp1B/Rd19, pDE1sp1B/HEmT-Rd19, and pDE1sp1B/HEmT-Rd19/DCN) were linearized with *Xmn* I and then cotransformed into *Escherichia coli* BJ5183 cells with linearized dE1-k35 to allow for homologous recombination, thus generating the oRd19 (Rd19-k35), oHEmT (HEmT-Rd19-k35), and oHEmT-DCN (HEmT-Rd19-k35/DCN) oncolytic Ad plasmids, respectively. The resultant homologously recombined Ad plasmids were digested with *Pac* I and transfected into HEK293 cells to generate the replication-competent Ads

oRd19, oHEmT, and oHEmT-DCN.

Replication-incompetent Ad and replication-competent oncolytic Ad were propagated in HEK293 cells and A549 cells, respectively. All viruses were obtained as previously described [21]. The numbers of viral particles (VP) were calculated from optical density measurements at 260 nm (OD_{260}), where 1 absorbency unit (OD_{260} = 1) indicated a concentration of 1.1×10^{12} VP/mL. Purified viruses were stored at −80°C until use.

Transduction efficiency analysis

To assess the transcriptional activity of the HmTE and HEmT promoters under normoxic and hypoxic conditions, fluorescence microscopy and fluorescence-activated cell sorting (FACS) analysis were carried out. Pancreatic cancer cells (MIA PaCa-2 and PANC-1) were transduced with GFP-expressing replication-incompetent Ad under the control of the HmTE or the HEmT promoter at an MOI of 50. At 48 hr post-transduction, cells were imaged using a fluorescence microscope (Carl Zeiss Inc., Thornwood, NY), and the GFP expression levels were quantified using a FACSCalibur analyzer (Becton-Dickinson, San Jose, CA). All FACS data were analyzed using CellQuest software (Becton-Dickinson). Approximately 10,000 events were counted for each sample.

To assess the cancer specificity of the CMV and HEmT promoters, fluorescence microscopy and FACS analysis were carried out. Cells were transduced with GFP-expressing Ad under the control of the CMV promoter or the HEmT promoter at MOIs of 5, 20, and 50. At 48 hr post-transduction, cells were imaged by fluorescence microscopy, and the GFP expression level was quantified using a FACSCalibur analyzer and CellQuest software. Approximately 10,000 events were counted for each sample.

MTT assay

To evaluate the extent to which HEmT-regulated oncolytic Ad (oHEmT) selectively kills cancer cells, pancreatic cancer cells (MIA PaCa-2 and PANC-1) and normal cells (NPCs and HDFs) seeded in 24-well plates were infected with oHEmT (or oRd19 as the cognate control) at an MOI of 2 under either normoxic or hypoxic conditions. At 60 hr post-infection, 200 μL of 3-(4,5-dimethylthiazol-2-yl)-2,5-diphenyl-tetrazolium bromide (MTT; Sigma, St. Louis, MO) in phosphate-buffered saline (PBS; 2 mg/mL) was added to each well. After 4 hr of incubation at 37°C, the supernatant was discarded from each well, and the precipitate was dissolved in dimethylsulfoxide. The absorbance of each well at 540 nm was then read on a microplate reader. All assays were performed in triplicate. The number of living cells in the untreated cell group

was analyzed in an identical manner as a negative control.

To evaluate the extent to which DCN-expressing oncolytic Ad (oHEmT-DCN) and the control oncolytic Ad (oHEmT) specifically kill cancer cells, and to determine whether this effect is dose-dependent, pancreatic cancer cells (MIA PaCa-2 and PANC-1) and normal cells (NPCs and HDFs) were grown in 24-well plates to 50-60% confluency. Next, cells were infected with oHEmT or oHEmT-DCN at an MOI of 1, 2, or 5. At 72 hr post-infection, the MTT assay was performed as described above.

In addition, the kinetics of pancreatic cancer cell killing by oncolytic Ads (oHEmT and oHEmT-DCN) was analyzed by the MTT assay. Specifically, upon reaching approximately 50-60% confluence, cells in 24-well plates were infected (MOI = 2) with oHEmT or oHEmT-DCN. The MTT assay was then performed at 24, 48, and 72 hr post-infection as described above.

Virus production assay

To assess the viral production of oncolytic Ads, pancreatic cancer cells and normal cells were seeded in 24-well plates at approximately 60% confluency and then infected with oRd19 or oHEmT at an MOI of 0.5 (pancreatic cancer cells) or 10 (normal cells). After 48 hr of incubation at 37°C under either normoxic or hypoxic conditions, supernatants and cell pellets were

collected and freeze-thawed three times to release internal virus. Real-time quantitative PCR (Q-PCR; TaqMan PCR detection; Applied Biosystems, Foster City, CA) was used to assess the number of viral genomes in each sample. Samples were analyzed in triplicate, and data were processed using the SDS 19.1 software package (Applied Biosystems).

Enzyme-linked immunosorbent assay (ELISA) measuring the levels of secreted decorin and TGF-β1 expression

Pancreatic cancer cells (MIA PaCa-2 and PANC-1) and normal cells (NPCs and HDFs) were seeded in 24-well plates at approximately 60% confluency and then infected with oHEmT-DCN at an MOI of 0.5 or 2. At 2 days post-infection, supernatants were collected by centrifugation at 15,000 × *g* for 10 min at 4°C, and the level of secreted DCN was assessed using an ELISA kit (Abcam, Ltd., Cambridge, UK).

To evaluate TGF-β1 expression in tumor tissue, tumor tissues were collected from mice treated with PBS or oncolytic Ads (ONYX-015, oHEmT, or oHEmT-DCN) at 30 days after the administration of the first viral treatment. Tumor tissues were homogenized in ice-cold RIPA buffer (Elipis Biotech, Taejeon, South Korea) containing a proteinase inhibitor cocktail (Sigma). Homogenates were then centrifuged in a high-speed microcentrifuge for 10 min,

after which total protein contents were determined using a BCA protein assay kit (Pierce, Rockford, IL). The level of TGF-β1 was measured by a conventional ELISA kit (R&D Systems, Minneapolis, MN).

Assessment of antitumor effects in an orthotopic model of human pancreatic cancer

MIA PaCa-2 cells (5×10^6), which stably express firefly luciferase, were injected into the pancreas of athymic nude mice. At 2 weeks post-implantation (day 0), mice were divided into four separate groups in order to receive intraperitoneal treatment of PBS, ONYX-015, oHEmT, or oHEmT-DCN (n=6 per group). Optical imaging was carried out every five days following the first treatment with an IVIS SPECTRUM instrument (Xenogen Corp., Alameda, CA). Image signals were quantitatively analyzed with IGOR-PRO Living Image software (Xenogen). At 30 days after the first treatment, tumors were collected, imaged, weighed, and sectioned.

Western blot analysis

To evaluate the levels of DCN and Ad E1A protein expression in tumor cell lysates from MIA PaCa-2 pancreatic orthotopic models, tumors were collected from Ad-treated mice at 30 days after the first viral treatment. Tumors

were homogenized in ice-cold RIPA buffer containing a proteinase inhibitor cocktail. The resultant homogenates were then centrifuged in a high-speed microcentrifuge for 10 min. Protein concentrations were determined by the BCA protein assay, and equal protein amounts (200 μg per sample) were resolved by sodium dodecyl sulfate-polyacrylamide gel electrophoresis. The proteins were electrotransferred to polyvinylidene fluoride membranes and incubated with goat anti-DCN antibody (Ab; R&D Systems), rabbit anti-Ad E1A Ab (Santa Cruz Biotechnology, Santa Cruz, CA), or rabbit anti-β-actin Ab (Cell Signaling Technology, Beverly, MA). Next, the membranes were incubated with secondary horseradish peroxidase-conjugated goat anti-rabbit IgG or mouse anti-goat IgG Ab (Cell Signaling). Immunoreactive bands were visualized via enhanced chemiluminescence (Amersham Pharmacia Biotech, Uppsala, Sweden). The expression levels of Ad E1A and DCN were semi-quantitatively analyzed using ImageJ software (National Institutes of Health, Bethesda, MD).

Histology and immunohistochemistry

Representative sections were stained with hematoxylin and eosin (H & E), picrosirius red, or Masson's trichrome and then examined using a light microscope (Carl Zeiss Inc.). Pancreatic tumor tissue sections and pancreatic

tumor spheroid sections were incubated at 4°C overnight with mouse anti-collagen type I (Abcam), mouse anti-collagen type III (Sigma), mouse anti-elastin (Sigma), mouse anti-fibronectin (Santa Cruz Biotechnology), rabbit anti-Ad E1A, or mouse anti-proliferating cell nuclear antigen (PCNA; DAKO, Glostrup, Denmark) primary Ab and then treated with an ABC-peroxidase kit (ChemMate DAKO Envision kit; DAKO, Carpinteria, CA). All slides were counterstained with Meyer's hematoxylin (Sigma), with the exception of picrosirius red-stained and Masson's trichrome (Sigma)-stained slides, which were counterstained with Harris' hematoxylin (Sigma). Collagen expression was detected by Masson's trichrome or picrosirius red staining, whereas the expression levels of Ad E1A, PCNA, type I and III collagen, elastin, and fibronectin in tumor tissues were detected by specific Ab staining. Expression levels were semi-quantitatively analyzed using MetaMorph® image analysis software (Universal Image Corp., Buckinghamshire, UK). Each result is expressed as the mean optical density of five different digital images.

Immunofluorescence staining

For immunofluorescence staining of Ad E1A and hypoxia-inducible factor 1α (HIF-1α), tumor sections were treated with rabbit anti-Ad E1A Ab or mouse anti-human HIF-1α Ab (Abcam) and incubated overnight at 4°C. Next,

the tumor sections were treated with Alexa Fluor 568 (red)-conjugated goat anti-rabbit IgG (Invitrogen, Carlsbad, CA) or Alexa Fluor 488 (green)-conjugated goat anti-mouse IgG (Invitrogen) Ab at room temperature for 1 hr. For counterstaining, the samples were incubated with 4,6-diamidino-2-phenylindole (Sigma). The slides were mounted with Vectashield mounting medium (Vector Laboratories, Burlingame, CA) and imaged under a confocal laser-scanning microscope (LSM510, Carl Zeiss MicroImaging, Thornwood, NY).

Terminal Deoxynucleotidyl Transferase dUTP Nick End Labeling Assay

Formalin-fixed and paraffin-embedded tissue sections (5-mm) were deparaffinized and rehydrated according to standard protocols [23]. Apoptosis was detected terminal deoxynucleotidyl transferase dUTP nick end labeling (TUNEL) assay (DeadEnd^{TM} Fluorometric TUNEL System; Promega, Madison, WI). Briefly, tissue sections were permeabilized with proteinase K (20 mg/mL) for 10 min at room temperature. Sections were then incubated with terminal deoxynucleotidyl transferase (TdT) and fluorescein-12-dUTP in TdT buffer at room temperature for 60 min and washed with TdT buffer. Finally, nuclei were counterstained with methyl green (Sigma). The samples were analyzed by light microscopy. The amount of apoptotic cells was semi-quantitatively analyzed

using MetaMorph® image analysis software. Each result is expressed as the mean optical density of five different digital images.

Preparation of pancreatic cancer patient-derived tumor spheroids

Primary pancreatic cancer tumors were obtained from patients with active-stage pancreatic cancer (n=3). Pancreatic cancer patient-derived tumor spheroids were prepared as previously described [14]. Plates containing the tumor spheroids were treated with oncolytic Ad (1×10^{10} VP of ONYX-015, oHEmT, or oHEmT-DCN) on days 1 and 4 and incubated at 37°C for 6 days. The treated tumor spheroids were then fixed with 10% formalin, embedded in paraffin, and cut into 5-μm-thick sections.

Statistical analysis

All data are expressed as mean ± standard deviation (SD). Statistical significance was determined by the two-tailed Student's *t*-test (SPSS 13.0 software; SPSS, Chicago, IL) and one-way ANOVA. Differences were considered statistically significant at $*P < 0.05$, $**P < 0.01$, and $***P < 0.001$.

III. RESULTS

Potent and tumor-selective activity of the HEmT promoter

The E2F and TERT promoters are established cancer-specific promoters that have been frequently utilized to endow cancer specificity to Ads [15, 17]. However, cancer-specific promoters alone cannot prevent the attenuation of Ad replication in the context of the hypoxic tumor microenvironment. To overcome hypoxia-induced downregulation of Ad E1A expression and enhance the promoter activity in cancer cells, we constructed two variants of a cancer-specific hybrid promoter, HRE/E2F/mTERT (HEmT) and HRE/mTERT/E2F (HmTE), by inserting 6 copies of the HRE upstream of either the E2F or mTERT promoter.

To compare the promoter activities of the HRE-harboring hybrid promoters, two different replication-incompetent Ads expressing GFP under the control of the HEmT or HmTE promoter were generated (dHmTE-GFP and dHEmT-GFP, respectively; **Figure 1A**). Pancreatic cancer cells (MIA PaCa-2 and PANC-1) were then transduced with either dHmTE-GFP or dHEmT-GFP, which were under the control of the hybrid promoters, for 48 hr. As shown in **Figure 2A** and **B**, dHEmT-GFP induced significantly higher GFP expression than dHmTE-GFP under normoxic conditions in both MIA PaCa-2 and PANC-

1 cells (**$P < 0.01$, ***$P < 0.001$, respectively), demonstrating the superior transcriptional activity of the HEmT promoter. More importantly, HEmT promoter activity was significantly enhanced under hypoxic conditions compared with normoxic conditions (***$P < 0.001$), demonstrating that insertion of the HRE enhancer upstream of a cancer-specific hybrid promoter can enhance Ad-mediated transgene expression under hypoxic conditions. Based on these results, the HEmT promoter was selected as a more potent promoter than the HmTE promoter and was utilized in subsequent experiments.

To assess the cancer selectivity of the HEmT promoter, pancreatic cancer cells (MIA PaCa-2 and PANC-1) or normal cells (NPCs and HDFs) were transduced with replication-incompetent GFP-expressing Ad under the control of either the CMV or HEmT promoter (dCMV-GFP and dHEmT-GFP, respectively). As shown in **Figure 3A** and **B**, both dCMV-GFP and dHEmT-GFP conferred a dose-dependent increase in relative GFP expression in pancreatic cancer cells. In contrast, negligible GFP expression was observed in dHEmT-GFP-transduced normal cells, even at a high multiplicity of infection (MOI) (50). In contrast, dCMV-GFP induced dose-dependent GFP expression in normal cells. Of particular note, dHEmT-GFP induced 31.9-fold and 72.0-fold lower GFP expression than dCMV-GFP at an MOI of 50 in NPC and HDF cells, respectively (***$P < 0.001$). These results demonstrate that the HEmT

promoter is highly cancer cell-selective, exhibits good transcriptional activity in tumor cells, and drives only minimal transcriptional activity in normal cells.

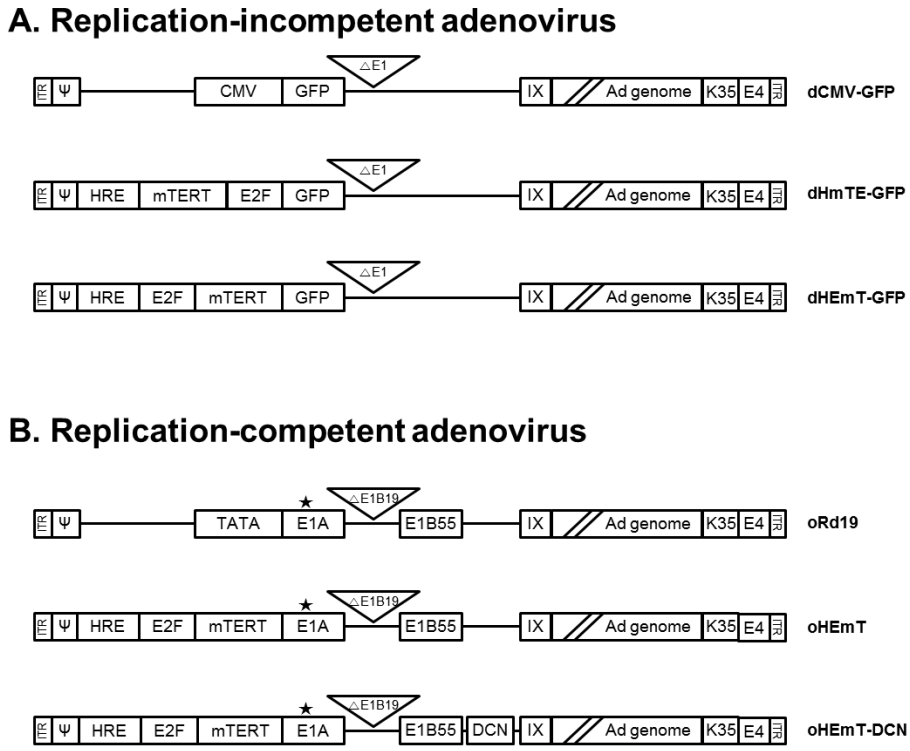

Figure 1. Construction of the Ads used in this study. (**A**) Replication-incompetent Ads expressing GFP under the control of the CMV, HmTE, or HEmT promoter. (**B**) Oncolytic Ads oRd19 contains a mutated E1A sequence and lacks the E1B 19kDa gene; E1A expression is controlled by the endogenous promoter. oHEmT contains a hypoxia-responsive enhancer and cancer-specific promoter (HEmT), which replaces the endogenous E1A promoter of oRd19. oHEmT-DCN contains the sequence encoding DCN in the E1 region of oHEmT.

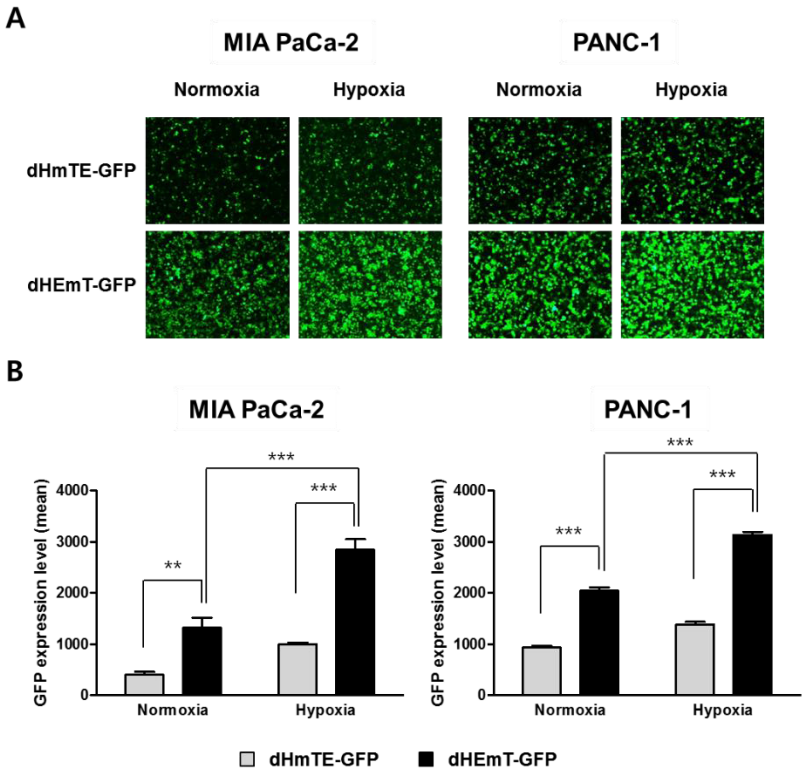

Figure 2. Levels of GFP expression driven by the HmTE or HEmT promoter in human pancreatic cancer cell lines (MIA PaCa-2 and PANC-1). Cells were transduced with Ads expressing GFP under the control of the HmTE or HEmT promoter (dHmTE or dHEmT) at an MOI of 50 under normoxic or hypoxic conditions. Fluorescence images (**A**) and quantitative FACS analysis (**B**) of GFP expression. Expression was analyzed after 48 hr incubation at 37°C. Data shown are representative of three independent experiments, each performed in triplicate. Bars represent mean ± SD. $^{**}P < 0.01$ and $^{***}P < 0.001$.

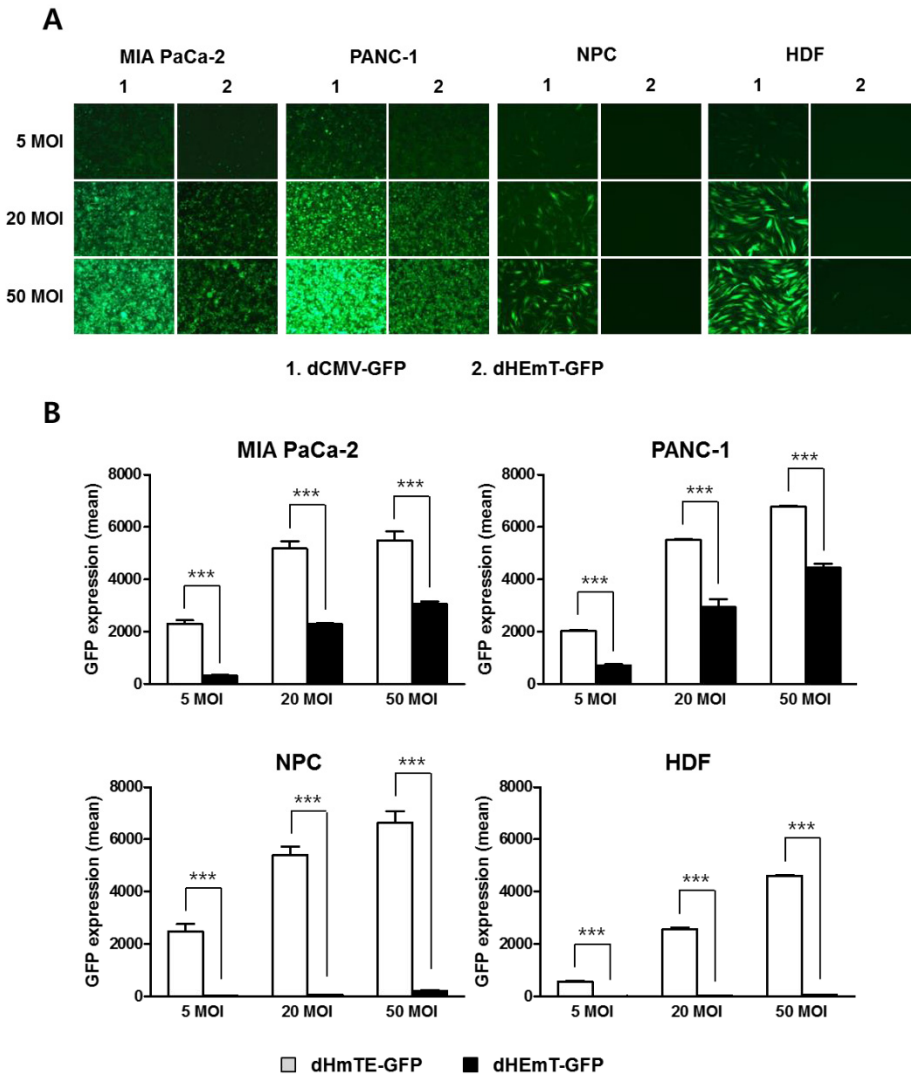

Figure 3. GFP expression driven by the cancer cell-specific promoter. Levels of GFP expression driven by the CMV or HEmT promoter (dCMV or dHEmT) in human pancreatic cancer (MIA PaCa-2 and PANC-1) and normal cell lines (NPC and HDF). Cells were transduced with Ads expressing GFP under the

control of the CMV or HEmT promoter at an MOI of 5, 20, or 50. Fluorescence images (**A**) and quantitative FACS analysis (**B**) of GFP expression. Expression was analyzed after 48 hr incubation at 37°C. Data shown are representative of three independent experiments, each performed in triplicate. Bars represent mean ± SD. ***$P < 0.001$.

Cancer cell-specific killing effect of HEmT promoter-regulated oncolytic Ad

We previously reported that oncolytic Ad containing mutated E1A retinoblastoma binding sites and harboring a deletion of the E1B 19kDa region (oRd19) exhibits potent cancer cell killing efficacy and good cancer specificity [21, 24]. In an effort to improve the cancer cell-specific viral replication and killing effects, we replaced the endogenous oRd19 promoter of the Ad E1A gene with the HEmT promoter, thus generating an oHEmT oncolytic Ad (**Figure 1B**).

To assess whether oHEmT oncolytic Ad could replicate and induce cell killing in a cancer-selective manner, cancer and normal cells were infected with oRd19 or oHEmT for 60 hr at an MOI of 2. As shown in **Figure 4**, oHEmT killed pancreatic cancer cells (MIA PaCa-2 and PANC-1) more efficiently than oRd19 under both normoxic and hypoxic conditions (***$P < 0.001$), whereas no cell killing was observed in normal cells (NPCs and HDFs). These findings indicate that oHEmT exhibits more potent cancer cell-specific killing efficacy than oRd19. Of particular note, oHEmT was not cytotoxic to normal cells under hypoxic conditions, indicating that incorporation of the HRE enhancer into the oHEmT promoter did not affect the cancer specificity of oncolytic Ad under hypoxic conditions. Specifically, oHEmT exhibited significantly higher cancer cell killing under hypoxic conditions than under normoxic conditions (18.1%

and 16.0% higher than in normoxic conditions in MIA PaCa-2 and PANC-1 cells, respectively; $^{**}P < 0.01$, $^{***}P < 0.001$). In contrast, no significant difference was detected in pancreatic cancer cells treated with oRd19 under hypoxic vs. normoxic conditions, indicating that oHEmT can overcome hypoxia-mediated attenuation of Ad E1A protein expression. Altogether, these results suggest that the HEmT promoter can enable replication-competent Ad to overcome hypoxia-mediated attenuation of viral replication and preferentially induce potent cancer cell killing.

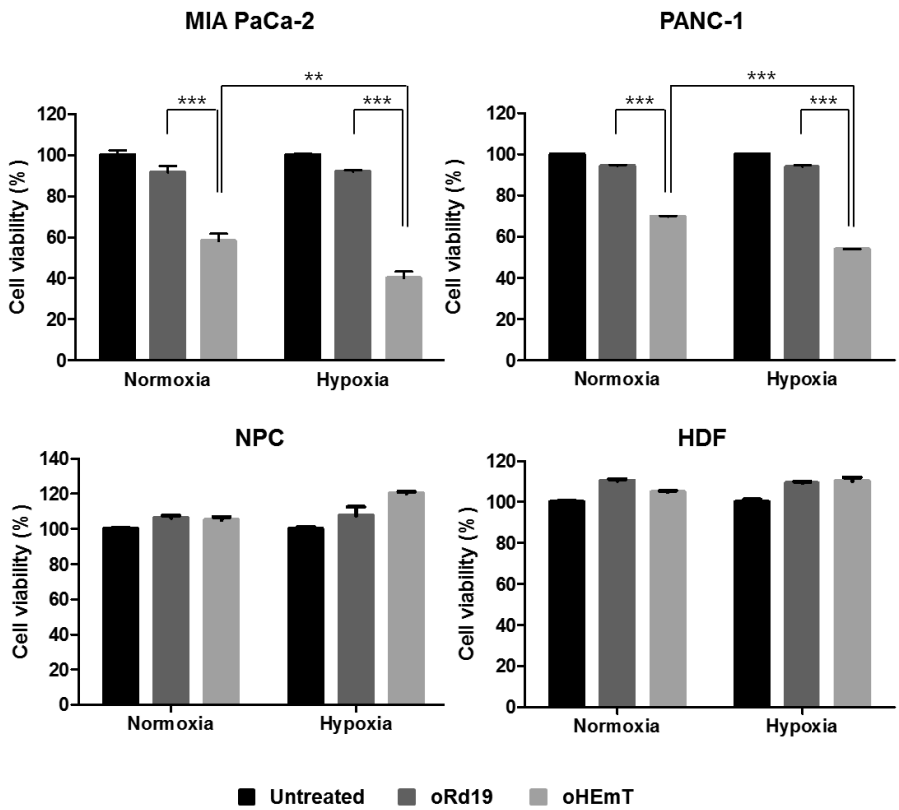

Figure 4. Cancer cell killing efficacy of oRd19 and oHEmT under normoxic and hypoxic conditions. Pancreatic cancer and normal cells were treated with oRd19 or oHEmT at an MOI of 2. Cell viability was assessed by the MTT assay. The viability of untreated cells was set to 100%. Data shown are representative of three independent experiments, each performed in triplicate. Bars represent mean ± SD. $^{**}P<0.01$ and $^{***}P < 0.001$.

Cancer cell-restricted replication of Ads controlled by the HEmT promoter

To assess whether oHEmT-induced cytotoxicity was dependent on viral replication, pancreatic cancer cells were infected for 48 hr at an MOI of 0.5 with oHEmT or its cognate control, oRd19 (**Figure 5**). In MIA PaCa-2 cells, oHEmT exhibited 2.1-fold and 4.6-fold higher viral production than oRd19 under normoxic and hypoxic conditions, respectively (**$P < 0.01$, ***$P < 0.001$). Similar results were observed in PANC-1 cells. These results indicate that the activity of the HEmT promoter is superior in both normoxic and hypoxic conditions to that of the endogenous Ad E1A promoter. Furthermore, viral replication of oHEmT was significantly lower than, or similar to, that of oRd19 in NPCs and HDFs at a high MOI (10), indicating that HEmT promoter-driven viral replication is highly cancer-specific. Taken together, these results demonstrate that the HEmT promoter can induce cancer-specific and proficient viral replication of oncolytic Ad under both normoxic and hypoxic conditions.

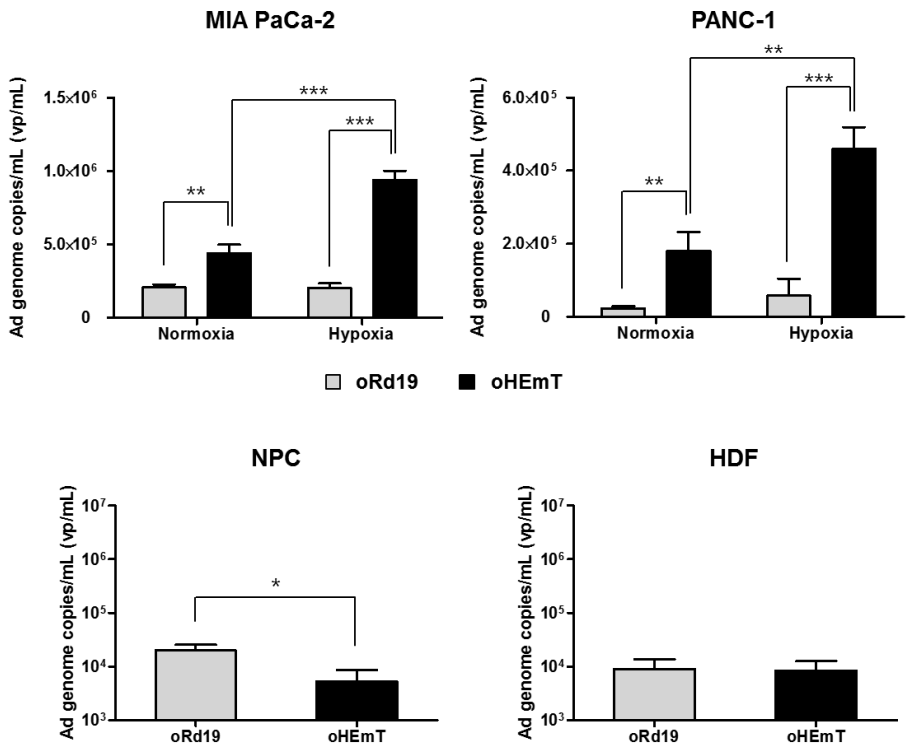

Figure 5. Viral production of oRd19 and oHEmT. Cells were treated with oRd19 or oHEmT at an MOI of 0.5 (pancreatic cancer cells) or 10 (normal cells). Viral production was assessed by Q-PCR at 48 hr after infection. Data shown are representative of three independent experiments, each performed in triplicate. Bars represent mean ± SD. **P*<0.05, ***P*<0.01, and ****P* < 0.001.

Cancer cell-specific expression of DCN by oHEmT-DCN

Desmoplasia, a prominent pathological attribute of pancreatic cancer, is marked by a dramatic increase in the proliferation of fibroblasts and increased deposition of ECM components [25]. Aberrant deposition of ECM components affects the overall elasticity and interstitial fluid pressure of the tumor, which can contribute to chemoresistance and poor viral distribution [14, 25]. To maximize the therapeutic efficacy of oncolytic Ad for the treatment of pancreatic tumors, we generated an HEmT promoter-driven oncolytic Ad expressing DCN (oHEmT-DCN). Our rationale for generating this Ad was that DCN can degrade aberrant ECM components such as collagen, elastin, and fibronectin (**Figure 1B**).

To assess whether oHEmT-DCN could induce cancer cell-specific expression of DCN, pancreatic cancer and normal cells were infected with oHEmT-DCN at an MOI of 0.5 or 2, and culture supernatants were examined for DCN secretion by ELISA. As shown in **Figure 6**, a dose-dependent increase in DCN expression was observed in pancreatic cancer cells infected with oHEmT-DCN (***$P < 0.001$). In marked contrast, only negligible DCN expression was detected in normal cells. Taken together, these results indicate that oHEmT-DCN can efficiently express DCN in a cancer cell-restricted manner, presumably due to the HEmT promoter-mediated cancer-specific

replication of oncolytic Ad.

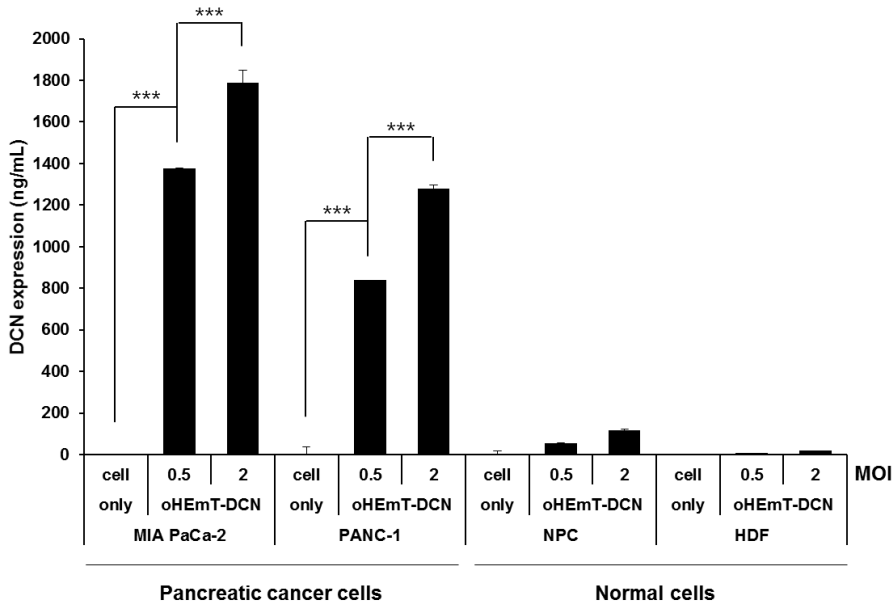

Figure 6. DCN expression in pancreatic cancer and normal cells infected with oHEmT-DCN. Cells were treated with oHEmT-DCN at an MOI of 0.5 or 2. DCN expression was assessed at 48 hr after infection by DCN ELISA. Data shown are representative of three independent experiments, each performed in triplicate. Bars represent mean ± SD. ***P<0.001.

Enhanced cancer cell-specific killing of DCN-expressing oncolytic Ad

We have previously reported that DCN-expressing Ad shows increased viral dissemination and greater cytotoxicity than control Ad by inducing apoptosis [14]. To determine whether oHEmT-DCN can more efficiently induce killing of pancreatic cancer cells than oHEmT, an MTT assay was performed to assess cell viability at various time points (**Figure 7**) and after infection with different MOIs (**Figure 8**). Both oHEmT and oHEmT-DCN elicited a time-dependent increase in pancreatic cancer cell killing efficacy, indicating that both oncolytic Ads replicate efficiently and induce cancer cell death. Importantly, oHEmT-DCN was significantly more cytotoxic to cancer cells than oHEmT at all time points (*$P < 0.05$, **$P < 0.01$, ***$P < 0.001$). Furthermore, the magnitude of difference in cancer cell killing efficacy was greater at later time points, suggesting that replication of oHEmT-DCN and subsequent amplification of DCN expression contributed to the potent cytopathic effect.

As shown in **Figure 8**, both oHEmT and oHEmT-DCN exhibited dose-dependent cytotoxicity to pancreatic cancer cells. Importantly, oHEmT-DCN was significantly more cytotoxic to cancer cells than oHEmT at all doses in MIA PaCa-2 and PANC-1 cells, further implying that oncolytic Ad-mediated expression of DCN enhances the potency of oncolytic Ad (***$P < 0.001$).

Furthermore, both oncolytic Ads induced only negligible cell death in normal cells, indicating that DCN expression is not detrimental to normal cells, and that DCN-mediated cell killing is cancer-selective. This result is consistent with a previous report in which DCN-mediated induction of apoptosis was shown to be cancer-specific [14]. Altogether, these results demonstrate that DCN expression mediated by oHEmT-DCN enhances the dose-dependent and time-dependent cytotoxicity of oncolytic Ad, which occurs specifically in cancer cells.

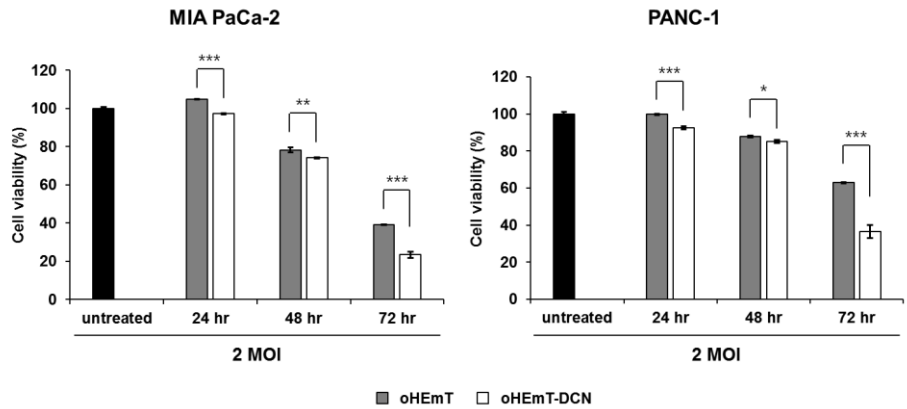

Figure 7. Cancer cell killing efficacy of oHEmT and oHEmT-DCN at various time points. Pancreatic cancer and normal cells were treated with oHEmT or oHEmT-DCN. The MTT assay was carried out at various time points (24-72 hr). The viability of untreated cells was set to 100%. Data shown are representative of three independent experiments, each performed in triplicate. Bars represent mean ± SD. **P*<0.05, ***P*<0.01, and ****P* < 0.001.

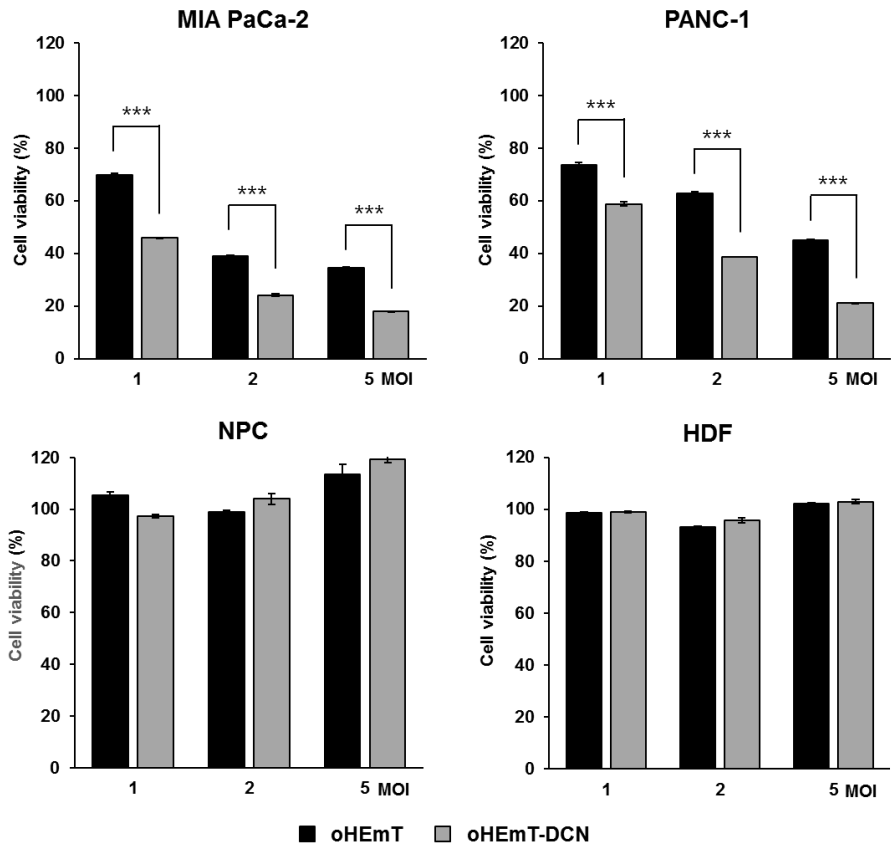

Figure 8. Cancer cell killing efficacy of oHEmT and oHEmT-DCN after infection with different MOIs. Pancreatic cancer and normal cells were treated with oHEmT or oHEmT-DCN. The MTT assay was carried out after treatment with various MOIs (1-5). The viability of untreated cells was set to 100%. Data shown are representative of three independent experiments, each performed in triplicate. Bars represent mean ± SD. ***$P < 0.001$.

Therapeutic efficacy of oHEmT and oHEmT-DCN in orthotopic pancreatic cancer

Orthotopic tumor models are emerging as a prominent model of cancer progression; moreover, the microenvironment of orthotopic tumors closely emulates that of clinical tumors [26, 27]. To evaluate the therapeutic potential of oHEmT-DCN against pancreatic cancer, we assessed the extent to which oncolytic Ads (oHEmT or oHEmT-DCN) could inhibit tumor growth in an orthotopic pancreatic cancer model. As a control, we used ONYX-015, a clinically approved oncolytic Ad. To monitor and visualize the growth of the orthotopic tumors in real time, orthotopic pancreatic tumors were established by injecting firefly luciferase-expressing MIA PaCa-2 pancreatic cancer cells into the pancreas of Balb/c nude mice. Tumor growth was then monitored by bioluminescence optical imaging.

As shown in **Figure 9** and **10**, the orthotopic pancreatic tumors continued to grow for up to 30 days after the initial treatment in PBS-treated, ONYX-015-treated, or oHEmT-treated mice. In contrast, oHEmT-DCN treatment resulted in a markedly lower tumor growth rate (***$P < 0.001$ versus PBS; **$P < 0.01$ versus ONYX-015, oHEmT). At 30 days after the initial treatment, the increase in total flux of PBS-treated, ONYX-015-treated, oHEmT-treated, and oHEmT-DCN-treated mice averaged 22.2, 24.9, 14.7, and

1.4-fold higher than the initial measurement, respectively. Surprisingly, ONYX-015 (which is clinically approved) did not suppress tumor growth, suggesting that the highly aggressive nature of orthotopic pancreatic tumors renders them refractory to treatment with ONYX-015. In marked contrast, both oHEmT and oHEmT-DCN suppressed tumor growth more effectively than ONYX-015, implying that HEmT promoter-driven oncolytic Ads are highly effective for the treatment of pancreatic tumors. Importantly, oHEmT-DCN inhibited tumor growth to a significantly greater extent than oHEmT, suggesting that oncolytic Ad-mediated DCN expression enhances the antitumor efficacy of oncolytic Ad (*$P < 0.05$, ***$P < 0.001$). Similarly, tumor weight measurements indicated that oHEmT-DCN was a more potent inhibitor of tumor growth than ONYX-015 or oHEmT, further supporting our conclusion that oHEmT-DCN is well-suited for the treatment of aggressive pancreatic tumors (**Figure 10**; ***$P < 0.001$ versus ONYX-015 and *$P < 0.05$ versus oHEmT).

To further investigate the mechanisms behind the antitumor effects of the different oncolytic Ads, Western blotting was performed to analyze the levels of Ad E1A and DCN expression in the tumors. As shown in **Figure 11**, oHEmT and oHEmT-DCN induced markedly higher expression of Ad E1A in tumor tissue than ONYX-015, implying that the HEmT promoter induces high

levels of viral replication in pancreatic tumors. Importantly, oHEmT-DCN induced 2.1-fold and 4.1-fold higher expression of Ad E1A and DCN, respectively, compared with oHEmT. This finding suggests that the potent antitumor efficacy of oHEmT-DCN was mediated by active viral replication and DCN expression in tumor tissue.

The TGF-β signaling pathway plays a critical role in the disease progression of cancer. This pathway regulates cell growth, differentiation, migration, and also induces the epithelial-to-mesenchymal transition (EMT) [28]. DCN has been reported to suppress the biological activity of TGF-β by preventing TGF-β binding to its receptor [14, 29]. Therefore, we performed ELISA to assess whether DCN expression mediated by oncolytic Ads affects the intratumoral expression level of TGF-β. As shown in **Figure 11**, the intratumoral expression level of TGF-β was significantly suppressed (by 32.6% and 26.8%) following treatment with oHEmT-DCN compared with the PBS and oHEmT treatments, respectively (**$P < 0.01$, ***$P < 0.001$). In contrast, no reduction of TGF-β expression was observed in ONYX-015-treated tumor tissue. Together, these results demonstrate that DCN expression is positively correlated with the suppression of TGF-β expression, and the potent antitumor efficacy of oHEmT-DCN was mediated by efficient viral replication, DCN expression, and subsequent downregulation of TGF-β.

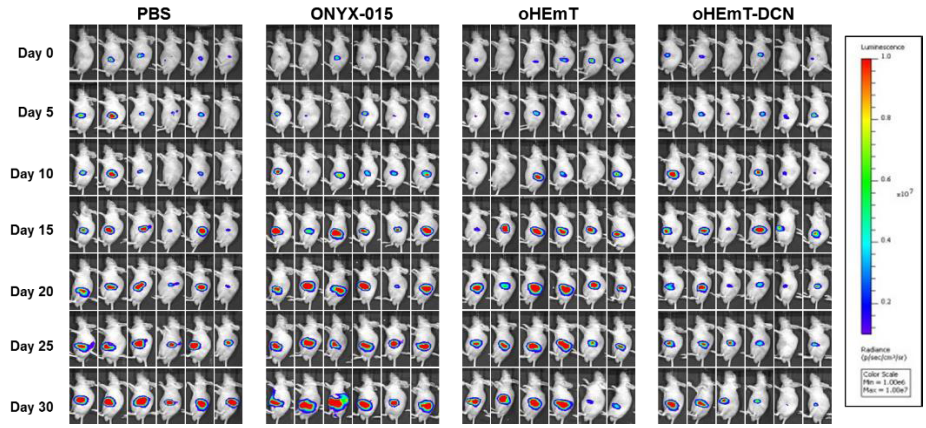

Figure 9. Potent tumor growth inhibition by DCN-expressing oncolytic Ad in a pancreatic orthotopic tumor xenograft model. Nude mice with MIA PaCa-2 orthotopic pancreatic tumors were intraperitoneally injected with PBS, ONYX-015, oHEmT, or oHEmT-DCN at two-day intervals. Firefly luciferase expression was monitored every 5 days after treatments using an IVIS imaging system.

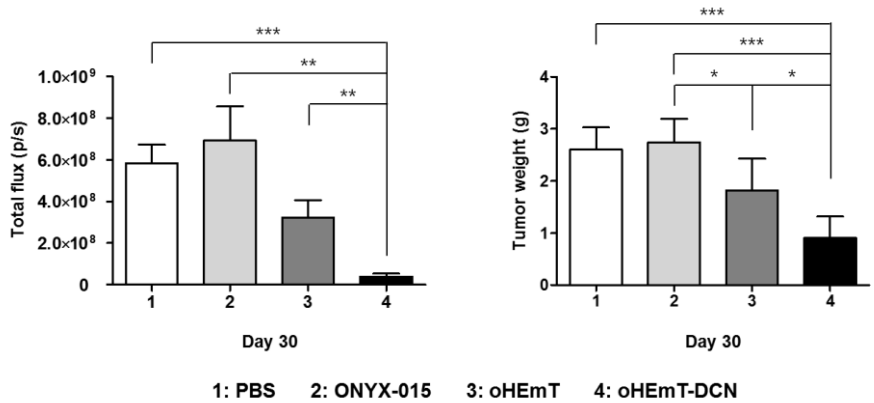

Figure 10. Quantification of bioluminescence signals and tumor weight. Bioluminescence signals were calculated in total flux of photons/second (p/s) after background subtraction from the region of interest. Tumors were harvested at 30 days following the first treatment and measured. Data are presented as mean ± SD. **P*<0.05, ***P*<0.01, and ****P* < 0.001.

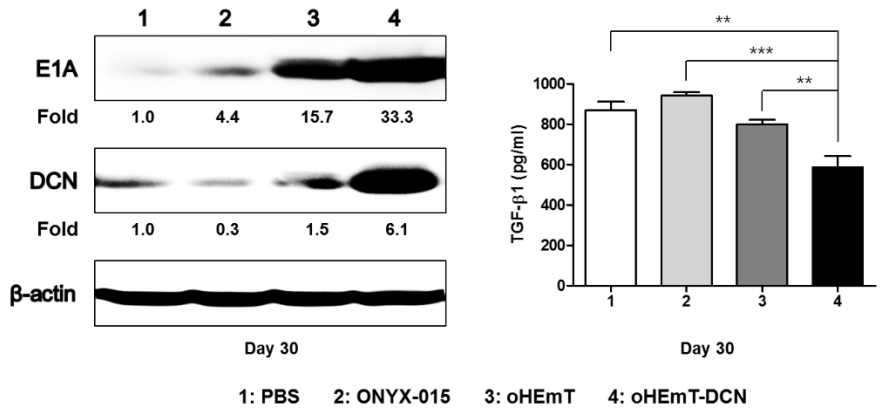

Figure 11. Protein expression in tumor tissue. Tumor tissues were lysed to generate total protein extracts. Western blotting and TGF-β1 ELISA were performed using the resultant tumor lysates. Data are presented as mean ± SD. $^{**}P<0.01$ and $^{***}P < 0.001$.

Histologic, TUNEL, and immunohistochemical characterization

The antitumor efficacy of the intraperitoneally administered oncolytic Ads was further investigated by histological and immunohistochemical analyses. H & E staining revealed a marked reduction in the number of viable tumor cells and more extensive necrotic regions in oHEmT-treated and oHEmT-DCN-treated tumors compared with PBS-treated and ONYX-015-treated tumors (**Figure 12**). Importantly, most of the oHEmT-DCN-treated tumor tissue was necrotic, whereas necrotic lesions were detected only in the central region of the oHEmT-treated tumor tissue, indicating that oHEmT-DCN can disperse through tumor tissue more effectively than oHEmT. Moreover, no necrosis was observed in normal tissues adjacent to the oHEmT-DCN-treated tumor tissues, suggesting that oHEmT-DCN preferentially induces necrosis in tumors.

Ad E1A staining revealed that the oHEmT-DCN-treated tumors exhibited markedly higher accumulation of Ad, through a greater area of the tumor, than ONYX-015-treated or oHEmT-treated tumors, indicating that expression of DCN facilitates viral replication and spreading within solid tumors. Consistent with the H & E staining results, no Ad E1A staining was observed in the surrounding normal tissues. This finding further confirms that the therapeutic effect of oHEmT-DCN is highly cancer-specific, and that tumor cell necrosis is induced by efficient viral replication-mediated cytolysis.

Tumor cell proliferation was markedly attenuated in oHEmT-DCN-treated tumors, as assessed by PCNA staining, Furthermore, a markedly higher percentage of tumor cells was undergoing apoptosis in oHEmT-DCN-treated tumors compared with PBS-treated, ONYX-015-treated, or oHEmT-treated tumors, as assessed by the TUNEL assay. Of particular interest, the induction level of apoptosis was positively correlated with viral replication, suggesting that high expression of DCN induced by active replication of oHEmT-DCN contributes to the induction of apoptosis in tumor tissue.

Hypoxia, a hallmark of the tumor microenvironment, has been reported to attenuate replication of oncolytic Ad [10], leading to insufficient therapeutic efficacy in hypovascular regions of solid tumors. Therefore, we examined the extent of replication of oncolytic Ads in hypoxic tumor regions. As shown in **Figure 13**, high levels of oHEmT and oHEmT-DCN replication were observed in hypoxic tumor regions, whereas no detectable accumulation of ONYX-015 was observed. The levels of oHEmT and oHEmT-DCN viral particles in hypoxic tumor regions were similar to those observed in normoxic regions. This finding demonstrates that the HREs upstream of the cancer-specific promoter can be transactivated by HIF-1α, which is overexpressed under hypoxia, to overcome hypoxia-mediated downregulation of Ad E1A expression. Importantly, oHEmT-DCN was distributed over a larger area and

more virus was observed under hypoxic conditions compared with oHEmT, indicating that DCN-mediated apoptosis facilitates viral dispersion throughout desmoplastic pancreatic tumors.

DCN has been shown to inhibit TGF-β activity, which plays a critical role in aberrant ECM deposition and the subsequent acquisition of resistance toward therapeutics in pancreatic tumors. Thus, we next assessed the effect of DCN-expressing oncolytic Ad on the ECM in orthotopic pancreatic tumors via histological and immunohistochemical staining. Masson's trichrome and picrosirious red staining of pancreatic tumor sections revealed that collagen deposition was significantly decreased in oHEmT-DCN-treated tumors compared with ONYX-015-treated or oHEmT-treated tumors. As shown in **Figure 14**, tumors treated with oHEmT-DCN contained less collagen compared with those treated with PBS, ONYX-015, or oHEmT (**$P < 0.01$, ***$P < 0.001$). Furthermore, oHEmT-DCN-treated tumors exhibited significantly attenuated accumulation of major ECM components such as type I collagen, type III collagen, elastin, and fibronectin compared with those treated with PBS, ONYX-015, or oHEmT. This finding indicates that oncolytic Ad-mediated expression of DCN effectively degrades overexpressed ECM components in pancreatic tumors (**Figure 15;** *$P < 0.05$, **$P < 0.01$, or ***$P < 0.001$). Taken together, these results indicate that oHEmT-DCN can efficiently degrade ECM,

overcome hypoxia-mediated downregulation of Ad E1A expression, and exhibit potent antitumor efficacy against highly desmoplastic pancreatic tumors.

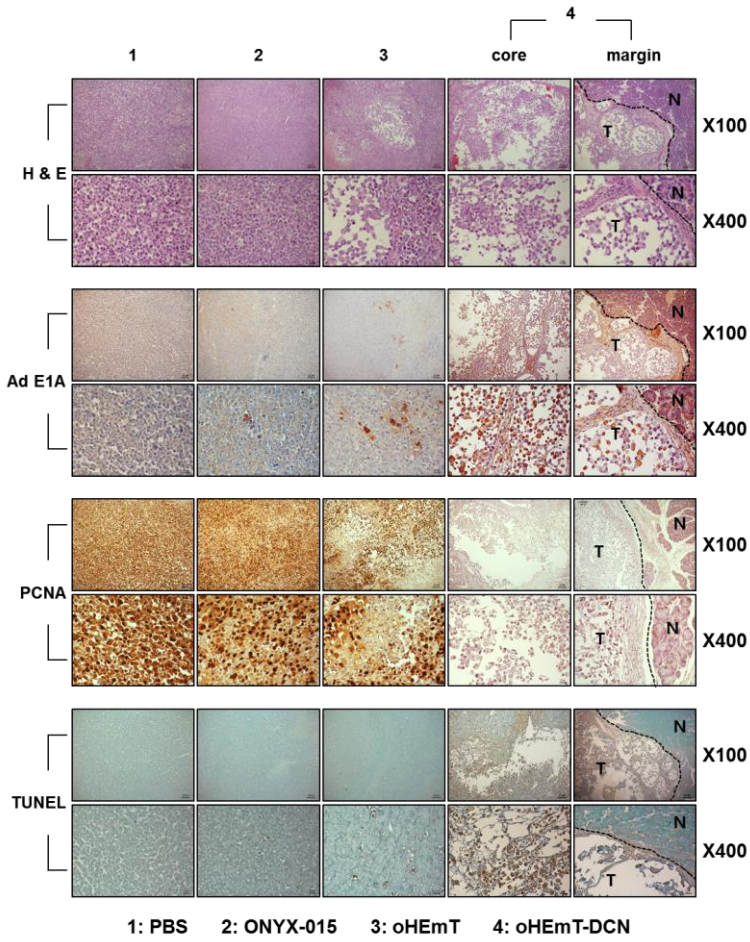

Figure 12. Histologic, TUNEL, and immunohistochemical staining of pancreatic cancer tissue. H & E staining, Ad E1A and PCNA immunohistochemical staining, and TUNEL assay results from pancreatic cancer tissue. Original magnification: ×100 and ×400. The tumor (T) and normal (N) tissues are separated with a dotted line in the oHEmT-DCN-treated group.

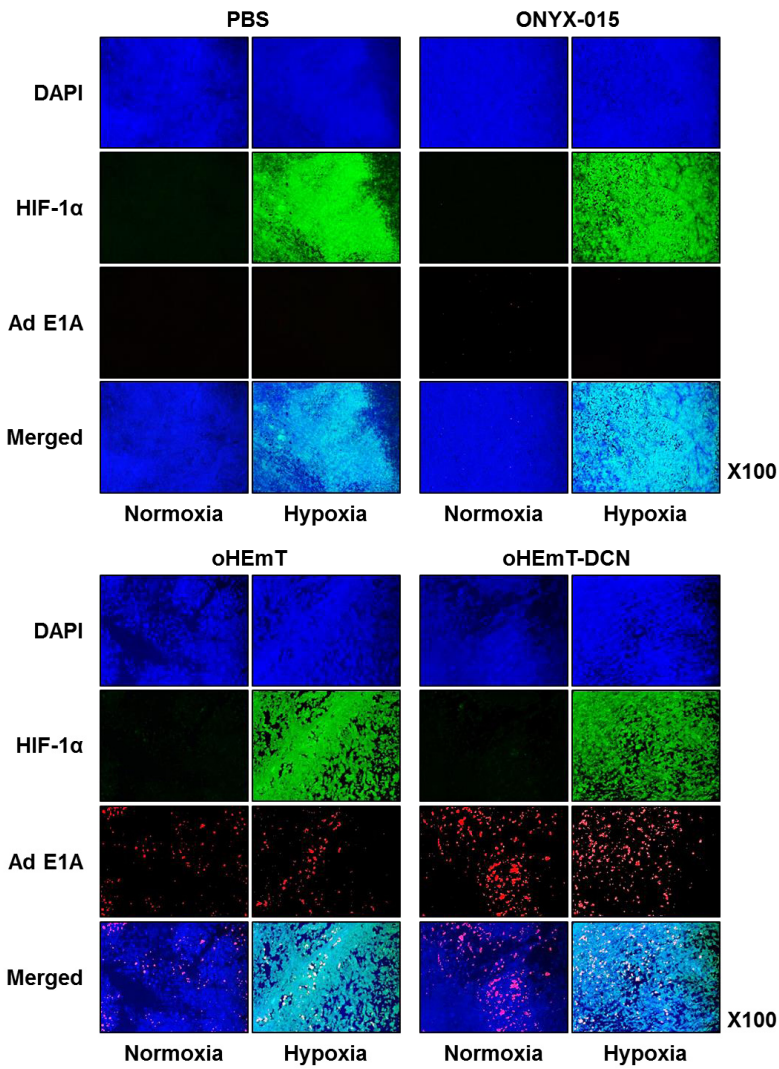

Figure 13. Replication of Ad in normoxic and hypoxic tumor regions. Tumor sections were stained with anti-Ad E1A Ab to examine viral replication (red). HIF-1α Ab were used to visualize hypoxic regions (green). Normoxic and hypoxic regions are both visible.

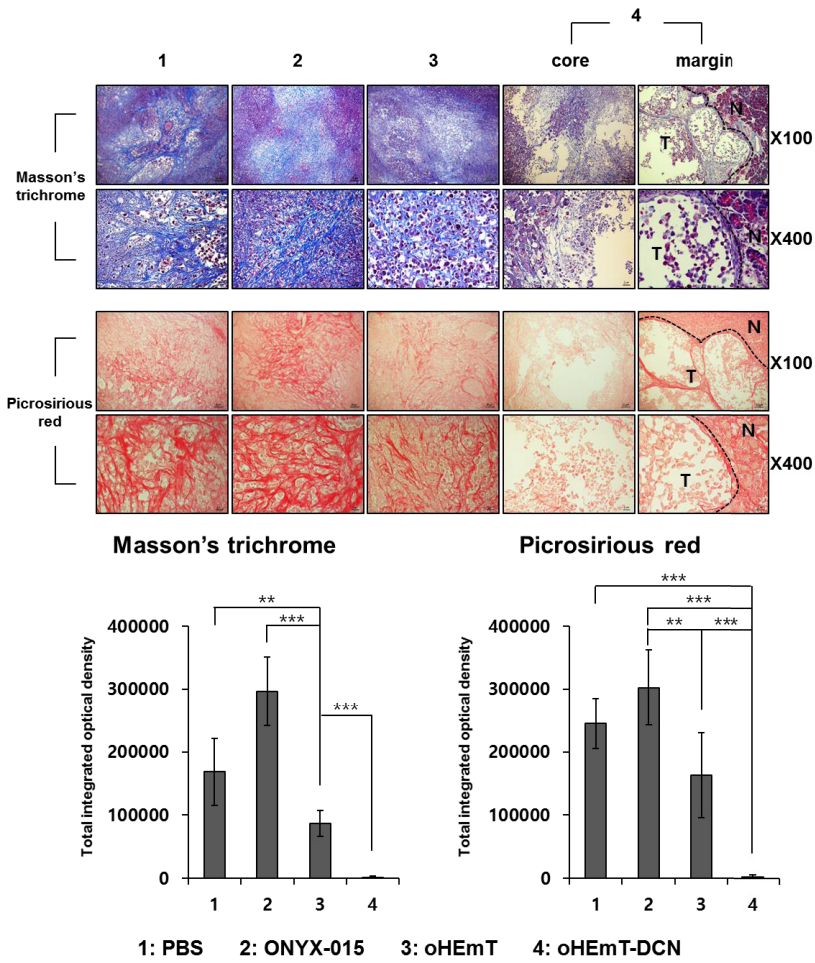

Figure 14. Masson's trichrome and picrosirius red staining of pancreatic cancer tissue. Collagen expression was analyzed semi-quantitatively from the resultant images. Original magnification: ×100 and ×400. The tumor (T) and normal (N) tissues are separated with a dotted line in the oHEmT-DCN-treated group. Data are presented as mean ± SD. **P*<0.05, ***P*<0.01, and ****P* < 0.001.

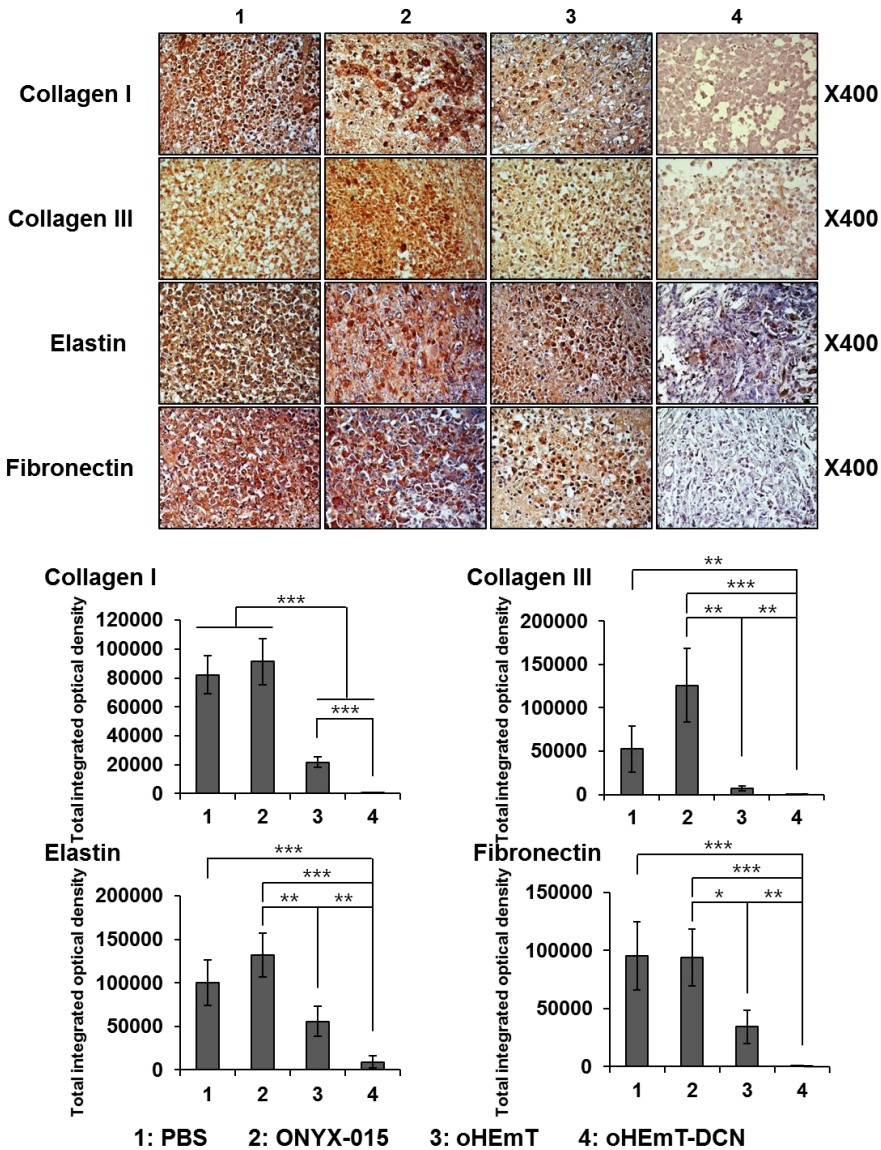

Figure 15. Expression of ECM components in pancreatic cancer tissue. Reduced protein levels of ECM components including collagen type I and III,

elastin, and fibronectin were observed in pancreatic cancer tissue treated with oHEmT-DCN compared with tissues treated with the other Ads. Semi-quantitative image analysis was performed to measure the protein levels of type I and III collagen, elastin, and fibronectin. Significantly reduced levels of type I collagen, type III collagen, elastin, and fibronectin were observed in pancreatic cancer tissue treated with oHEmT-DCN than in the tumor tissues treated with the control viruses. Original magnification: ×400. Data are presented as mean ± SD. $*P<0.05$, $**P<0.01$, and $***P < 0.001$.

Therapeutic efficacy of oHEmT-DCN in patient-derived pancreatic cancer organoid cultures

Although orthotopic tumor models closely emulate tissue-specific disease progression of clinical tumors, orthotopic implantation in immunodeficient mice does not completely recapitulate tumorigenesis in humans because the tumor microenvironments are not equivalent [30]. In this regard, 3D organoid culture of patient tumors, an approach that mimics the ECM components and complex cell heterogeneity of clinical tumors, is a promising model for the evaluation of novel therapeutics [31-34]. To take advantage of this model system, pancreatic tumor spheroids derived from patient samples were cultured and treated with PBS, ONYX-015, oHEmT, or oHEmT-DCN for 6 days. As shown in **Figure 16**, PBS-treated patient-derived pancreatic tumor spheroids were primarily composed of a thick and dense layer of ECM components, similar to orthotopic pancreatic tumors (**Figure 17**). This finding indicates that 3D tumor spheroids and orthotopic models both closely emulate the desmoplastic attributes of clinical pancreatic tumors. In good agreement with our results from the orthotopic pancreatic tumor model, oHEmT-DCN induced efficient degradation of major ECM components, attenuated proliferation of tumor cells, induced apoptosis in tumor cells, and exhibited proficient viral dissemination in patient-derived tumor spheroids

(**Figure 16-18**). Together, these results suggest that oHEmT-DCN induces potent antitumor effects by overcoming hypoxia-mediated downregulation of Ad E1A expression and desmoplasia in patient-derived tumor spheroids, suggesting oHEmT-DCN as a promising candidate for future clinical trials targeting aggressive and desmoplastic pancreatic cancer.

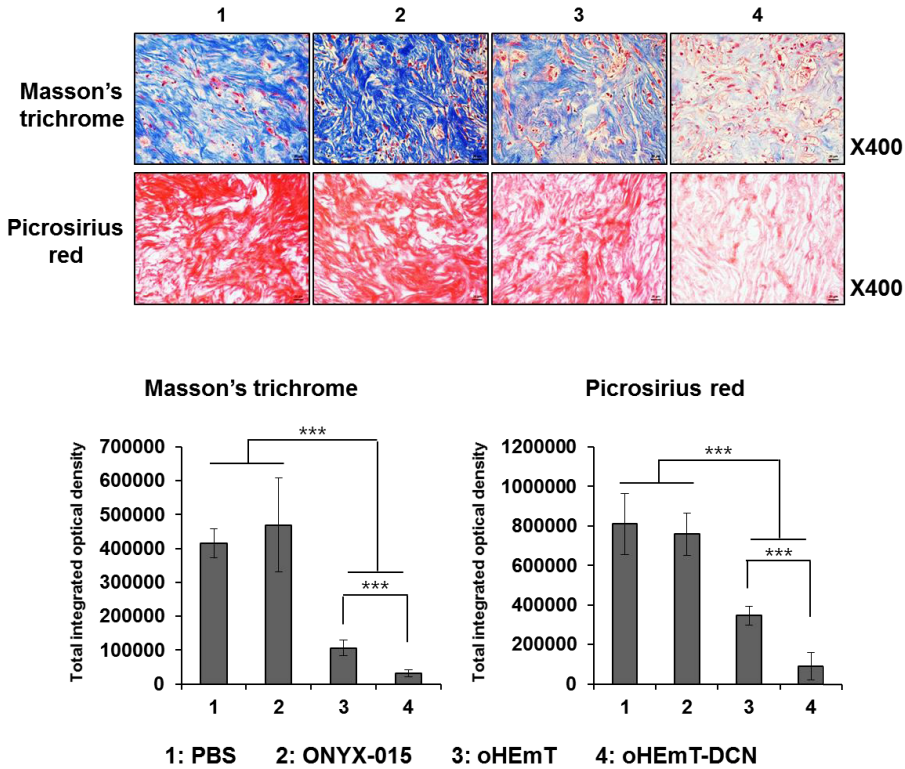

Figure 16. Histological staining of pancreatic cancer patient-derived tumor spheroids. Masson's trichrome and Picrosirius red staining of pancreatic cancer patient-derived tumor spheroids treated with PBS, ONYX-015, oHEmT, or oHEmT-DCN. Collagen expression was analyzed semi-quantitatively. Original magnification: ×400. Bars represent mean ± SD. ***$P < 0.001$.

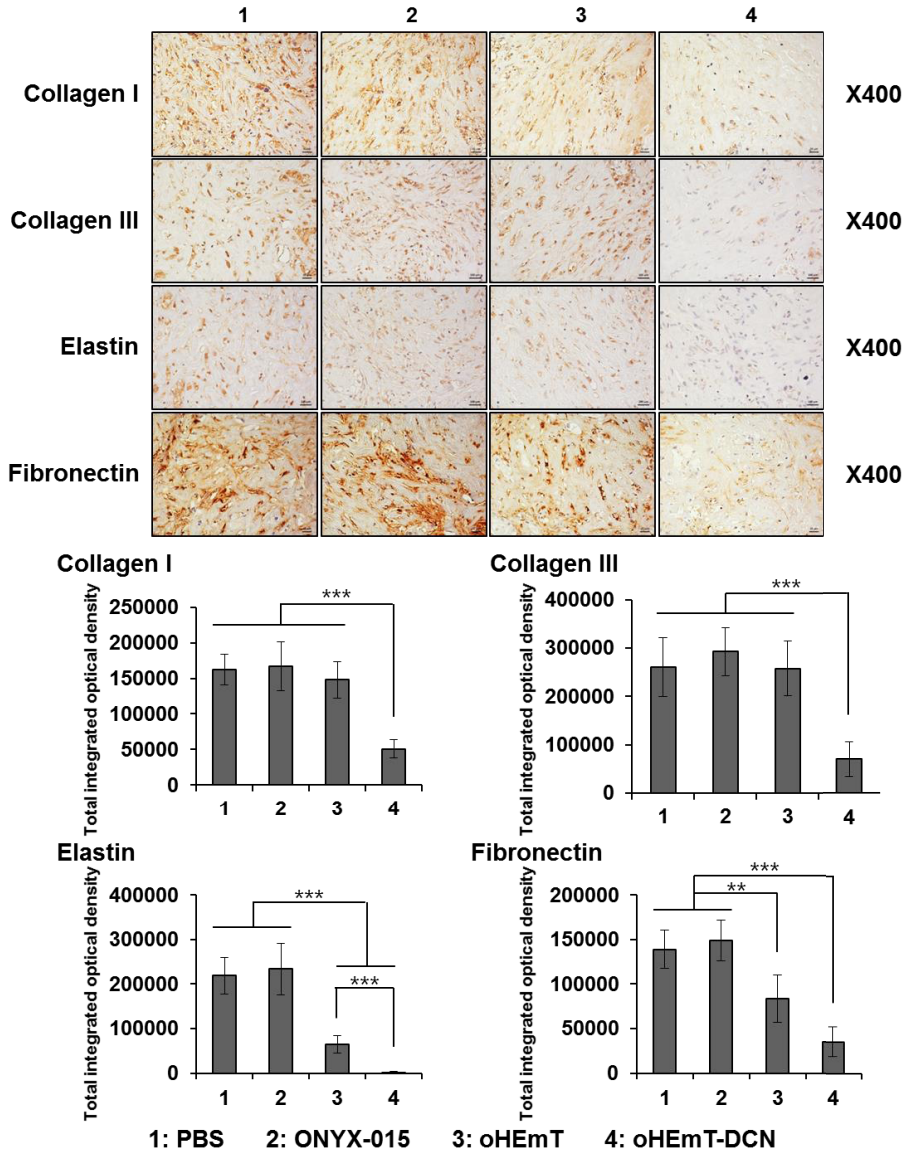

Figure 17. Immunohistochemical staining of pancreatic cancer patient-derived tumor spheroids for ECM components. Reduced protein levels of various ECM

components including collagen type I and III, elastin, and fibronectin were observed in primary pancreatic tumor spheroids treated with oHEmT-DCN compared with spheroids treated with the other Ads. Type I and III collagen, elastin, and fibronectin protein levels were analyzed semi-quantitatively. Significantly reduced levels of type I collagen, type III collagen, elastin, and fibronectin were observed in primary pancreatic tumor spheroids treated with oHEmT-DCN compared with spheroids treated with control viruses. Original magnification: ×400.

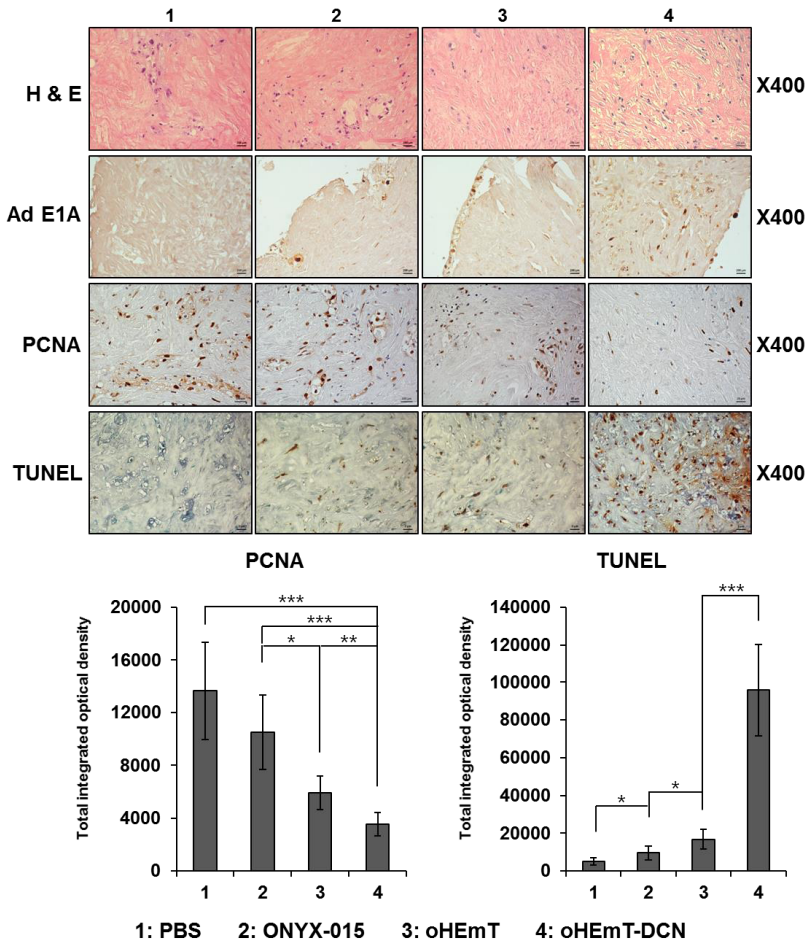

Figure 18. Histologic, TUNEL, and immunohistochemical staining of pancreatic cancer patient-derived tumor spheroids. H & E staining, Ad E1A and PCNA immunohistochemical staining, and TUNEL assay results from primary pancreatic tumor spheroids. Original magnification: ×400. PCNA expression and TUNEL assay images were analyzed semi-quantitatively. Bars represent mean ± SD. **P*<0.05, ***P*<0.01, and ****P* < 0.001.

IV. DISCUSSION

Pancreatic cancer is associated with the worst prognosis of all gastrointestinal malignancies [35-37]. The major reasons for these poor outcomes are late diagnosis and poor therapeutic efficacy of conventional treatments, which are due to the nonspecific symptoms and aggressive tumor biology, respectively. Histologically, pancreatic cancer tumors are extremely stroma-rich and hypovascular. Indeed, most of the pancreatic tumor mass consists of ECM components, such as collagen, desmin, fibronectin, and hyaluronic acid [38-40]. Aberrant accumulation of ECM in the tumor microenvironment is a major obstacle hindering the success of conventional treatments against pancreatic cancer. Gemcitabine, a standard chemotherapeutic prescribed for the treatment of pancreatic cancer, can only prolong life expectancy by 6 months. The inefficiency of this therapeutic has been shown to be due to poor drug permeation into ECM-rich tumors [25, 41].

Another critical hurdle for the effective treatment of pancreatic cancer is hypoxia, which refers to the low partial pressure of oxygen and subsequent acidosis that frequently occur in the tumor microenvironment [42]. HIF-1α, a potent regulator of the homeostatic transcriptional response to hypoxia, is significantly overexpressed in pancreatic cancer [43, 44]. Importantly, HIF-1α stimulates transcription of genes that contain HREs in their promoters.

Therefore, transcriptional regulation via a hypoxia- inducible promoter is frequently employed to target the hypoxic tumor microenvironment.

In the present report, we generated two variants of HRE-harboring, cancer-selective hybrid promoters (HEmT and HmTE). The levels of transgene expression driven by the HEmT promoter and by the HmTE promoter were both significantly enhanced under hypoxic conditions, indicating that the HRE enhancer enhances promoter activity under hypoxic conditions. Importantly, the HEmT promoter induced higher Ad transgene expression than the HmTE promoter under both normoxic and hypoxic conditions, demonstrating that the level of transcriptional activity of a given hybrid promoter is affected by the order in which the promoter components are inserted into the Ad genome (**Figure 2A** and **B**). Since the HEmT promoter demonstrated superior promoter activity to that of the HmTE promoter, we chose to extensively characterize the therapeutic efficacy of HEmT-harboring Ads. In addition to exhibiting enhanced transcription in hypoxic conditions, HEmT-driven expression of GFP was highly cancer-specific. This finding indicates that our novel HEmT hybrid promoter is a good candidate for regulating Ad E1A gene expression of oncolytic Ad in a manner that endows cancer specificity (**Figure 3A** and **B**). Oncolytic Ad replicating under the control of the HEmT promoter (oHEmT) was highly cytotoxic to cancer cells and exhibited significant replication in a

highly cancer-specific manner under both normoxic and hypoxic conditions (**Figure 4** and **5**). These findings are in good agreement with our previous report, in which we demonstrated the cancer selectivity of HRE-mediated enhancement of oncolytic Ad transgene expression under hypoxic conditions [10]. Of note, oHEmT exhibited greater viral replication than oRd19, a control oncolytic Ad with the endogenous Ad promoter, in cancer cells. In contrast, no evident cytotoxicity was observed in normal cells, implying that the potent and cancer-specific killing effect of oHEmT is mediated by efficient and preferential replication of oncolytic Ad in cancer cells (**Figure 4** and **5**).

Current trends of oncolytic Ad development for clinical applications have focused on armed oncolytic Ads expressing anticancer therapeutic genes. Several clinical studies have evaluated the efficacy of these Ads against various types of cancers [45-47]. In the context of this strategy, we generated oncolytic Ad expressing DCN, a potent inducer of tumor cell apoptosis and ECM degradation, as a potential candidate for the treatment of desmoplastic pancreatic cancer. DCN-expressing oncolytic Ad (oHEmT-DCN) induced a dose-dependent increase in DCN expression in a cancer cell-specific manner (**Figure 6**). Furthermore, oHEmT-DCN exhibited dose-dependent cytotoxicity in a cancer cell-specific manner that was superior to that of its cognate control oncolytic Ad oHEmT, indicating that the dose-dependent increase in DCN

achieved with oHEmT-DCN was responsible for the enhanced anticancer effect (**Figure 8)**. Moreover, oHEmT-DCN was more highly cytotoxic than oHEmT, in a time-dependent manner, further demonstrating that amplification of DCN and oncolytic Ad via active viral replication resulted in potent cancer cell killing (**Figure 7)**. Of particular interest, only negligible oHEmT-DCN-induced DCN expression was detected in normal cells, and no cytotoxicity was observed, findings that are in good agreement with a previous report demonstrating that DCN-induced apoptosis was cancer-specific [48]. Similar results were observed *in vivo*; that is, oHEmT-DCN exhibited superior antitumor efficacy via DCN-mediated induction of apoptosis and active viral replication within highly aggressive and desmoplastic orthotopic pancreatic tumor tissue compared to its cognate control oHEmT (**Figure 9-12**). Furthermore, normal tissue adjacent to the tumor was not affected by oHEmT-DCN. These findings are in good agreement with previous reports demonstrating that DCN induces cancer-selective apoptosis but is not detrimental to normal cells, providing further support for the idea that low level expression level of Ad-mediated DCN in normal cells is not harmful [14, 26].

The ECM is a critical hurdle complicating oncolytic Ad-mediated gene therapy for the treatment of pancreatic cancer, since the coarse and dense ECM prevents penetration and dispersion of Ad into tumor tissue. TGF-β is a key

profibrotic cytokine that induces ECM accumulation in pancreatic tumors by inhibiting proteolytic enzymes. Decorin harbors a high-affinity binding site for TGF-β; thus, binding of decorin to TGF-β neutralizes its biological activity [13]. We found that TGF-β protein level was significantly reduced by oHEmT-DCN in orthotopic pancreatic tumor tissue, supporting the idea that decorin is a natural inhibitor of TGF-β (**Figure 11**). Importantly, DCN-mediated suppression of TGF-β following oHEmT-DCN treatment was positively correlated with attenuation in the expression levels of major ECM components, such as collagen types I & III, fibronectin, and elastin, indicating that oncolytic Ad-mediated expression of DCN can effectively degrade ECM components in tumor tissue via downregulation of the profibrotic cytokine TGF-β (**Figure 11, 14,** and **15**). In addition, the DCN expression level and extent of ECM component degradation were both positively correlated with Ad dispersion and accumulation within pancreatic tumors. These findings are in good agreement with a previous report, demonstrating that DCN enhances Ad penetration and distribution within solid tumors via ECM degradation [14]. Alternatively, induction of apoptosis has been reported to enhance viral dispersion within solid tumors by transferring Ad progeny virus to neighboring tumor cells via apoptotic bodies and attenuating intratumoral interstitial pressure [49]. In good agreement with this report, oHEmT-DCN potently induced apoptosis in tumor

tissue; furthermore, this effect was positively correlated with the extent of viral dispersion and replication within solid tumors. Together, these results demonstrate that oHEmT-DCN potently induces apoptosis and efficient degradation of ECM components, thereby resulting in high levels of viral dissemination and active replication within orthotopic pancreatic tumor tissue.

Hypovascularization within solid tumors has been demonstrated to suppress replication of oncolytic Ad, resulting in poor and uneven viral distribution in tumor tissue [11, 12]. The HRE enhancer, which binds to overexpressed HIF-1α under hypoxic conditions and induces transactivation of its downstream promoters, has been frequently employed to achieve tumor selectivity. Oncolytic Ad replicating under the control of our novel HRE-harboring cancer-specific hybrid promoter HEmT (oHEmT) showed enhanced viral replication under hypoxic conditions compared with normoxic conditions. Thus, our strategy was able to overcome hypoxia-induced downregulation of Ad E1A expression both *in vitro* and *in vivo* (**Figure 5** and **13**). Furthermore, the level of Ad E1A expression achieved with oHEmT-DCN was markedly higher than that achieved with ONYX-015 or its cognate control, oHEmT, in hypoxic tumor regions. Together, these results demonstrate that the combination of a hypoxia-responsive promoter with intratumoral expression of DCN can yield enhanced viral replication and dispersion of oHEmT-DCN in

hypovascular tumor regions, as well as in normoxic regions of ECM-rich pancreatic tumors.

3D organoid culture of primary patient tumors can provide a more accurate representation of the clinical tumor microenvironment compared with orthotopic xenograft models. Furthermore, 3D patient tumor spheroids retain their heterogeneous tumor cell populations as well as the complex network of cell-cell and cell-matrix interactions exhibited in clinical tumors, making this model a promising candidate for evaluating the penetration and action of novel therapeutics [50, 51]. In the present study, both orthotopic pancreatic tumors and tumor spheroids derived from patients with pancreatic cancer exhibited aberrantly high deposition of ECM components. These characteristics closely emulate the desmoplastic attributes of clinical pancreatic cancer described in previous literature (**Figure 14,** and **16)**. In both orthotopic tumors and primary patient spheroids, oHEmT-DCN effectively induced tumor cell apoptosis, ECM degradation, and dispersion of Ad in both normoxic and hypoxic tumor regions, leading to a potent tumoricidal effect.

In summary, we demonstrated that a novel DCN-expressing oncolytic Ad, oHEmT-DCN, can potently inhibit tumor growth through a multifunctional process. In this process, degradation of ECM, hypoxia responsiveness, and induction of apoptosis facilitate dispersion and active replication of oncolytic

Ad in both normoxic and hypoxic regions of desmoplastic pancreatic tumors that closely emulate clinical tumors. These findings suggest oHEmT-DCN as a promising therapeutic candidate for future clinical trials against aggressive pancreatic cancer.

V. CONCLUSION

In this study, our results demonstrate that oHEmT-DCN can potently inhibit tumor growth through a multifunctional process. In this process, ECM degradation, hypoxia responsiveness, and induction of apoptosis facilitate the permeation and replication of oncolytic Ad in both normoxic and hypoxic regions of desmoplastic pancreatic tumors. Our results indicate that our novel oncolytic Ad, oHEmT-DCN, is a promising therapeutic agent for the treatment of aggressive and highly desmoplastic pancreatic cancer.

REFERENCES

1. Malvezzi, M., et al., *European cancer mortality predictions for the year 2014.* Ann Oncol, 2014. **25**(8): p. 1650-6.
2. Siegel, R., D. Naishadham, and A. Jemal, *Cancer statistics, 2013.* CA Cancer J Clin, 2013. **63**(1): p. 11-30.
3. Laheru, D., B. Biedrzycki, and E.M. Jaffee, *Development of a cytokine-modified allogeneic whole cell pancreatic cancer vaccine*, in *Pancreatic Cancer*. 2013, Springer. p. 175-203.
4. Eager, R. and J. Nemunaitis, *Clinical development directions in oncolytic viral therapy.* Cancer gene therapy, 2011. **18**(5): p. 305-317.
5. Sinkovics, J. and J. Horvath, *New developments in the virus therapy of cancer: a historical review.* Intervirology, 1993. **36**(4): p. 193-214.
6. Toth, K., D. Dhar, and W.S. Wold, *Oncolytic (replication-competent) adenoviruses as anticancer agents.* Expert Opin Biol Ther, 2010. **10**(3): p. 353-68.
7. Xia, Z.J., et al., *Phase III randomized clinical trial of intratumoral injection of E1B gene-deleted adenovirus (H101) combined with cisplatin-based chemotherapy in treating squamous cell cancer of head and neck or esophagus.* Ai Zheng, 2004. **23**(12): p. 1666-70.
8. FAC., R.H.I.A., *A randomized phase III trial of talimogene laherparepvec (T-VEC) versus subcutaneous (SC) granulocyte-macrophage colonystimulating factor (GM-CSF) for the treatment (tx) of unresected stage IIIB/C and IV melanoma.* Journal of Clinical Oncology, 2013.
9. Erickson, L.A., et al., *Targeting the hypoxia pathway to treat pancreatic cancer.* Drug Des Devel Ther, 2015. **9**: p. 2029-31.
10. Kwon, O.J., et al., *A hypoxia- and {alpha}-fetoprotein-dependent oncolytic adenovirus exhibits specific killing of hepatocellular carcinomas.* Clin Cancer Res, 2010. **16**(24): p. 6071-82.

11. Shen, B.H. and T.W. Hermiston, *Effect of hypoxia on Ad5 infection, transgene expression and replication.* Gene Ther, 2005. **12**(11): p. 902-10.
12. Pipiya, T., et al., *Hypoxia reduces adenoviral replication in cancer cells by downregulation of viral protein expression.* Gene Ther, 2005. **12**(11): p. 911-7.
13. Yamaguchi, Y., D.M. Mann, and E. Ruoslahti, *Negative regulation of transforming growth factor-beta by the proteoglycan decorin.* Nature, 1990. **346**(6281): p. 281-4.
14. Choi, I.K., et al., *Effect of decorin on overcoming the extracellular matrix barrier for oncolytic virotherapy.* Gene Ther, 2010. **17**(2): p. 190-201.
15. Hemminki, O., et al., *Immunological data from cancer patients treated with Ad5/3-E2F-Delta24-GMCSF suggests utility for tumor immunotherapy.* Oncotarget, 2015. **6**(6): p. 4467-81.
16. Lanson, N.A., Jr., et al., *Replication of an adenoviral vector controlled by the human telomerase reverse transcriptase promoter causes tumor-selective tumor lysis.* Cancer Res, 2003. **63**(22): p. 7936-41.
17. Kim E, K.J., Shin HY, Lee H, Yang JM, Kin J, Sohn JH, Kim H, Yun co, *AdmTERTD19, a Conditional Replication Competent Adenovirus Driven by the Human Telomerase Promoter,Selectively Replicates in and Elicits Cytopathic Effect in a Cancer Cell-Specific Manner.* 2003.
18. *Immunological data from cancer patients treated with Ad5 3-E2F-Δ24-GMCSF suggests utility for tumor immunotherapy.* 2014.
19. Lee, J.S., et al., *A novel sLRP6E1E2 inhibits canonical Wnt signaling, epithelial-to-mesenchymal transition, and induces mitochondria-dependent apoptosis in lung cancer.* PLoS One, 2012. **7**(5): p. e36520.
20. Kim, E.K., et al., *Enhanced antitumor immunotherapeutic effect of B-cell-based vaccine transduced with modified adenoviral vector containing type 35 fiber structures.* Gene Ther, 2014. **21**(1): p. 106-14.
21. Kim, J., et al., *E1A- and E1B-Double mutant replicating adenovirus elicits enhanced oncolytic and antitumor effects.* Hum Gene Ther, 2007. **18**(9): p.

773-86.

22. Yoon, A.R., et al., *Markedly enhanced cytolysis by E1B-19kD-deleted oncolytic adenovirus in combination with cisplatin.* Hum Gene Ther, 2006. **17**(4): p. 379-90.
23. Yun, C.O., et al., *ADP-overexpressing adenovirus elicits enhanced cytopathic effect by induction of apoptosis.* Cancer Gene Ther, 2005. **12**(1): p. 61-71.
24. Kim, J., et al., *Evaluation of E1B gene-attenuated replicating adenoviruses for cancer gene therapy.* Cancer Gene Ther, 2002. **9**(9): p. 725-36.
25. Whatcott, C.J., et al., *Desmoplasia and chemoresistance in pancreatic cancer*, in *Pancreatic Cancer and Tumor Microenvironment*, P.J. Grippo and H.G. Munshi, Editors. 2012, Transworld Research Network Transworld Research Network.: Trivandrum (India).
26. Na, Y., et al., *Potent antitumor effect of neurotensin receptor-targeted oncolytic adenovirus co-expressing decorin and Wnt antagonist in an orthotopic pancreatic tumor model.* J Control Release, 2015. **220**(Pt B): p. 766-82.
27. Weber, H.L., et al., *A Novel CDC25B Promoter-Based Oncolytic Adenovirus Inhibited Growth of Orthotopic Human Pancreatic Tumors in Different Preclinical Models.* Clin Cancer Res, 2015. **21**(7): p. 1665-74.
28. Pickup, M., S. Novitskiy, and H.L. Moses, *The roles of TGFbeta in the tumour microenvironment.* Nat Rev Cancer, 2013. **13**(11): p. 788-99.
29. Lee, W.J., et al., *Decorin-expressing adenovirus decreases collagen synthesis and upregulates MMP expression in keloid fibroblasts and keloid spheroids.* Exp Dermatol, 2015. **24**(8): p. 591-7.
30. Qiu, W. and G.H. Su, *Development of orthotopic pancreatic tumor mouse models.* Methods Mol Biol, 2013. **980**: p. 215-23.
31. Hwang, C.I., et al., *Preclinical models of pancreatic ductal adenocarcinoma.* J Pathol, 2016. **238**(2): p. 197-204.
32. Boj, S.F., et al., *Organoid models of human and mouse ductal pancreatic cancer.* Cell, 2015. **160**(1-2): p. 324-38.

33. Whittle, J.R., et al., *Patient-derived xenograft models of breast cancer and their predictive power.* Breast Cancer Res, 2015. **17**: p. 17.

34. Malaney, P., S.V. Nicosia, and V. Dave, *One mouse, one patient paradigm: New avatars of personalized cancer therapy.* Cancer Lett, 2014. **344**(1): p. 1-12.

35. Singh, H.M., G. Ungerechts, and A.M. Tsimberidou, *Gene and cell therapy for pancreatic cancer.* Expert Opin Biol Ther, 2015. **15**(4): p. 505-16.

36. Siegel, R., D. Naishadham, and A. Jemal, *Cancer statistics, 2013.* CA: a cancer journal for clinicians, 2013. **63**(1): p. 11-30.

37. Yadav, D. and A.B. Lowenfels, *The epidemiology of pancreatitis and pancreatic cancer.* Gastroenterology, 2013. **144**(6): p. 1252-61.

38. Erkan, M., et al., *The role of stroma in pancreatic cancer: diagnostic and therapeutic implications.* Nat Rev Gastroenterol Hepatol, 2012. **9**(8): p. 454-67.

39. Neesse, A., et al., *Stromal biology and therapy in pancreatic cancer.* Gut, 2011. **60**(6): p. 861-8.

40. Wormann, S.M., et al., *The immune network in pancreatic cancer development and progression.* Oncogene, 2014. **33**(23): p. 2956-67.

41. Ying, J.E., L.M. Zhu, and B.X. Liu, *Developments in metastatic pancreatic cancer: is gemcitabine still the standard?* World J Gastroenterol, 2012. **18**(8): p. 736-45.

42. Vaupel, P., O. Thews, and M. Hoeckel, *Treatment resistance of solid tumors: role of hypoxia and anemia.* Med Oncol, 2001. **18**(4): p. 243-59.

43. Koong, A.C., et al., *Pancreatic tumors show high levels of hypoxia.* Int J Radiat Oncol Biol Phys, 2000. **48**(4): p. 919-22.

44. Ye, L.Y., et al., *Hypoxia-inducible factor 1alpha expression and its clinical significance in pancreatic cancer: a meta-analysis.* Pancreatology, 2014. **14**(5): p. 391-7.

45. Yoon, A., S. W Kim, and C.-O. Yun, *Armed Oncolytic Adenoviruses and Polymer-shielded Nanocomplex for Systemic Delivery.* Current Cancer

Therapy Reviews, 2015. **11**(3): p. 136-153.

46. Bramante, S., et al., *Oncolytic virotherapy for treatment of breast cancer, including triple-negative breast cancer.* Oncoimmunology, 2016. **5**(2): p. e1078057.
47. Kanerva, A., et al., *Antiviral and antitumor T-cell immunity in patients treated with GM-CSF-coding oncolytic adenovirus.* Clin Cancer Res, 2013. **19**(10): p. 2734-44.
48. Tralhao, J.G., et al., *In vivo selective and distant killing of cancer cells using adenovirus-mediated decorin gene transfer.* Faseb j, 2003. **17**(3): p. 464-6.
49. Mi, J., et al., *Induced apoptosis supports spread of adenovirus vectors in tumors.* Hum Gene Ther, 2001. **12**(10): p. 1343-52.
50. Longati, P., et al., *3D pancreatic carcinoma spheroids induce a matrix-rich, chemoresistant phenotype offering a better model for drug testing.* BMC Cancer, 2013. **13**: p. 95.
51. Kim, J.B., *Three-dimensional tissue culture models in cancer biology.* Semin Cancer Biol, 2005. **15**(5): p. 365-77.

ABSTRACT (in Korean)

종양 미세환경을 개선하는 데코린 발현 종양 특이적 살상 아데노바이러스의 개발 및 췌장암 모델에서의 항종양 효과 평가

<지도교수 최 인 홍>

연세대학교 대학원

나노메디칼협동과정

리 연

2013 년 말 발표된 국가 암 등록통계 자료에 따르면, 췌장암은 한국인 암 사망원인의 5 위로 조사된 암종 중 5 년 생존율이 가장 낮은 5%, 중앙생존기간은 5 개월에 불과한 가장 치명적 종양질환이다. 췌장암 환자의 90% 정도는 이미 근치적 수술을 시행할 수 없는 상태에서 발견되어 인체 암 중 예후가 가장 불량한 것으로 보고되었다. 또한 췌장암 환자의 항암제 반응률은 20% 내외에 불과할 뿐 아니라 조기에 항암제 내성이 발생하는 것으로 알려져 있다. 결합조직증식 반응(desmoplasia)이 활발하게 일어나는 췌장암 조직은 조직 내 증가된 저산소 조건과 과도하게 분포된 세포외기질(extracellular matrix)로 인해 종양의 악성도가 크게 증가될 뿐 아니라 약물의 침투 및 확산이 저해되고 이러한

췌장암 조직의 독특한 특성은 항암 치료제의 치료효과를 감소시키는 원인으로 작용한다. 그러므로 이러한 췌장암의 종양 미세환경을 표적할 수 있는 새로운 패러다임의 췌장암 치료제의 개발이 절실히 요구되는 실정이다.

따라서 본 연구에서는, 종양 특이적 살상 아데노바이러스의 저산소 조건에서의 복제능을 증가시키기 위해, 종양 살상 아데노바이러스인 Rd19-k35 에 종양 선택성을 높이고 저산소 조건에서 바이러스의 복제를 조절할 수 있는 HmTE 와 HEmT 프로모터를 도입하여 oHmTE(HmTE-Rd19-k35)와 oHEmT(HEmT-Rd19-k35)를 제작하였다. 췌장암 세포주에서 제작된 oHmTE 와 oHEmT 의 암세포 살상능 및 바이러스 증식능을 검증하여, oHmTE 에 비해 oHEmT 가 우수한 프로모터 활성을 나타내는 것을 확인하였다. 이러한 결과를 바탕으로, oHEmT 바이러스에 세포고사를 유도하고 세포외기질을 분해할 수 있는 데코린(DCN)유전자를 삽입하여 oHEmT-DCN 을 제작하고 이를 이용하여 췌장암 동소이식 동물모델 및 췌장암 환자 유래 종양조직에서 항종양 효과를 확인하였다. oHEmT-DCN 를 투여한 그룹에서 현재 시판되고 있는 종양 특이적 살상 아데노바이러스인 ONYX-015 또는 대조군인 oHEmT 를 투여한 그룹에 비해 현저히 향상된 항종양 효과가 나타남을 확인하였다. 뿐만 아니라 췌장암 조직에서 HEmT 프로모터에 의해 바이러스가 저산소 환경을 효과적으로 표적하여 저산소 조건에서의 바이러스 복제저하가 개선됨을 확인하였고, 종양조직 내에서 oHEmT-DCN 에 의한 치료유전자 DCN 의 발현 증가, TGF-β 의 발현 감소, 바이러스 분포 및 복제 증가, 췌장암 조직 내의 세포외기질 분해 증가, 그리고 종양조직 특이적 세포고사의 증가 등을 통해 결과적으로

우수한 항종양 효과가 유도됨을 확인하였다. 따라서 데코린을 발현하는 종양 선택적 살상 아데노바이러스는 종양 미세환경의 저산소 조건 및 세포외기질을 효과적으로 표적하고 증대된 항종양 효과를 유도하므로 안전하고 효과적인 췌장암 치료제로 적용될 수 있을 것으로 사료된다.

핵심되는 말: 종양 특이적 살상 아데노바이러스; 췌장암; 데코린; 저산소; 결합조직증식; 종양 특이적 프로모터; 세포외기질

PUBLICATION LIST

1. Choi IK, **Li Y**, Oh E, Kim J, Yun CO; Oncolytic adenovirus expressing IL-23 and p35 elicits IFN-γ- and TNF-α-co-producing T cell-mediated antitumor immunity. PLoS One. 2013 Jul 3;8(7):e67512. (IF: 3.534)

2. Choi WI, Kim MY, Jeon BN, Koh DI, Yun CO, **Li Y**, Lee CE, Oh J, Kim K, Hur MW; Role of promyelocytic leukemia zinc finger (PLZF) in cell proliferation and cyclin-dependent kinase inhibitor 1A (p21WAF/CDKN1A) gene repression. J Biol Chem. 2014 Jul 4;289(27):18625-40. (IF: 4.6)

3. Na Y, Choi JW, Kasala D, Hong J, Oh E, **Li Y**, Jung SJ, Kim SW, Yun CO; Potent antitumor effect of neurotensin receptor-targeted oncolytic adenovirus co-expressing decorin and Wnt antagonist in an orthotopic pancreatic tumor model. J Control Release. 2015 Dec 28;220(Pt B):766-82. (IF: 7.705)

4. Min B, Park H, Lee S, **Li Y**, Choi JM, Lee JY, Choi YD, Kwon YG, Lee HW, Bae SC, Yun CO, Chung KC; CHIP-mediated degradation of transglutaminase 2 negatively regulates tumor growth and angiogenesis in renal cancer. Oncogene, 2015 Nov 16. (IF: 8.559)

5. Yoon AR, Kasala D, **Li Y**, Hong J, Lee W, Jung SJ, Yun CO; Antitumor effect and safety profile of systemically delivered oncolytic adenovirus complexed with EGFR-targeted PAMAM-based dendrimer in orthotopic lung tumor model. J Control Release. 2016 Mar 4. pii: S0168-3659(16)30110-9. (IF: 7.705)

6. El-Shemi AG, Ashshi AM, Na Y, **Li Y**, Basalamah M, Al-Allaf FA, Oh E, Jung BK, Yun CO; Combined therapy with oncolytic adenoviruses encoding TRAIL and IL-12 genes markedly suppressed human hepatocellular carcinoma both in vitro and in an orthotopic transplanted mouse model. J Exp Clin Cancer Res. 2016 May 6;35(1):74 (IF: 3.271)

7. **Li Y**, Hong J, Oh JE, Yoon AR, Yun CO; Potent antitumor effect of tumor microenvironment-targeted oncolytic adenovirus against desmoplastic pancreatic cancer. Cell Death Differ. 2016. Under review (IF: 8.218)